

UC San Diego

UC San Diego Electronic Theses and Dissertations

Title

Modeling FOXP1 Syndrome: Enhancing model Accuracy and Biomimicry

Permalink

<https://escholarship.org/uc/item/5r41n7f8>

Author

Iyer, Sneha

Publication Date

2022

Peer reviewed|Thesis/dissertation

UNIVERSITY OF CALIFORNIA SAN DIEGO

Modeling *FOXG1* Syndrome: Enhancing model Accuracy and Biomimicry

A Thesis submitted in partial satisfaction of the requirements for the degree

Master of Science

in

Bioengineering

by

Sneha Iyer

Committee in charge:

Professor Alysson R. Muotri, Chair

Professor Adam Engler, Co-chair

Professor Brian Aguado

2023

The Thesis of Sneha Iyer is approved, and it is acceptable in quality
and form for publication on microfilm and electronically:

University of California San Diego

2023

DEDICATION

I dedicate this thesis to my family - my parents, my sister and my grandma. They have all been my pillars of strength throughout my journey in grad school, despite being 8000 miles away. They have always been extremely supportive of my goals and dreams and I'm really grateful for that. I would also like to thank my friends for being there for me, their encouragement has been invaluable to me. Love you all!

TABLE OF CONTENTS

Thesis Approval Page	iii
Dedication	iv
List of Abbreviations	vi
List of Figures	ix
List of Tables	xi
Acknowledgements	xii
Abstract of the Thesis	xiii
Chapter 1	1
Chapter 2	17
Chapter 3	25
Discussion	36
Materials and Methods	39
Supplementary Figures	45
References	49

LIST OF ABBREVIATIONS

<i>FOXP1</i>	Forkhead box protein G1
WNT	Wingless/ Integrated signaling pathway
Cre	cAMP Response element
iPSCs	Induced pluripotent stem cells
3-D	Three-dimensional
CRISPR	Clustered regularly interspaced short palindromic Repeats
Cas9	Caspase 9 enzyme
NSCLC	Non-Small Cell Lung Cancer
HER2	human epidermal growth factor receptor 2
MeCP2	Methyl-CpG binding protein 2 in
Oct4	Gene for POU class 5 homeobox 1 protein
Sox2	Gene for Sex determining region -box transcription factor (<i>homo sapiens</i>)
Klf4	Gene for Krüppel-like factor 4 transcription factor (<i>homo sapiens</i>)
c-Myc	Gene for MYC proto-oncogene transcription factor (<i>homo sapiens</i>)
EB	Embryoid bodies
NPC	Neural progenitor cells
FGF	Fibroblast growth factor

EGF	Epidermal Growth factor
NANOG	Gene for Nanog-box protein (<i>homo sapiens</i>)
LIN28	Gene for RNA binding protein that promotes pluripotency in iPSCs
RNA	Ribonucleic Acid
qPCR	quantitative Polymerase Chain Reaction
PAX6	Pair box protein Pax-6
TBP	TATA-box binding protein (<i>homo sapiens</i>)
GAPDH	glyceraldehyde-3-phosphate dehydrogenase (<i>homo sapiens</i>)
DAPI	4',6-diamidino-2-phenylindole.
Nestin	Protein: neuroepithelial stem cell protein.
SMAD	SMAD (mothers against decapentaplegic) family transcription factors
BMP	Bone Morphogenetic Proteins
TGF- β	Transforming growth factor-beta
RNA-Seq	Ribonucleic Acid Sequencing
NSCs	Neural Stem Cells
LXH2	LIM/homeobox protein (<i>homo sapiens</i>)
CNS	Central Nervous System tissues
hPSC	Human pluripotent stem cell

2-D	Two-dimensional
N-cadherin	Neural calcium dependent adhesion proteins. Form adherens junctions between neural cells.
MIP	Maximum Intensity Projection
BDNF	Brain derived neurotrophic factor
GDNF	Glial cell derived neurotrophic factor
cAMP	Cyclic adenosine monophosphate
DMEM	Dulbecco's Modified Eagle Medium
bFGF	basic epidermal growth factor
DPBS	Dulbecco's Phosphate Buffered Saline
BSA	Bovine Serum Albumin
OCT	Optimal Temperature Compound
PFA	Paraformaldehyde
cDNA	complementary Deoxyribonucleic acid
MEM-NEAA	Modified Eagle Non-Essential Amino Acids
ECM	Extracellular Matrix

LIST OF FIGURES:

Figure No.	Figure Title	Page Number
1	Workflow diagram for cortical organoid generation	6
2	Workflow diagram showing the process of making cortical neural organoids from patient fibroblasts.	7
3	Characterization of p.Gly169Glyfs*23 iPS Cells	9
4	Relative expression of <i>FOXG1</i> and <i>LHX2</i> in control and mutant organoids	9
5	Size difference between Control and Mutant organoids	10
6	Immunostaining of control and <i>FOXG1</i> mutant organoids	12
7	Percentage of <i>FOXG1</i> positive cells in control and <i>FOXG1</i> mutant organoids	13
8	Cortical organoids with multiple rosette morphology	15
9	Immunostaining of control and <i>FOXG1</i> organoids +/- WNTi	19
10	Percentage of <i>FOXG1</i> positive cells in control and <i>FOXG1</i> mutant organoids +/- WNTi	20
11	Relative expression (RT-qPCR) of <i>FOXG1</i> in 15-day old Control and <i>FOXG1</i> mutant patient derived organoids with XAV-939 treatment	21
12	Schematic showing analogy between rosettes and neural tube formation	26
13	Schematic showing the design of the micropattern dish	

	consisting of a glass bottom with micropatterns of 500 um diameters. iPSCs are seeded onto it.	28
14	Schematic of organoid development throughout 10 days	29
15	IF images of Single rosette organoid from WT83C6 cell line	30
16	IF images of <i>FOXG1</i> mutant cell line p.Gly224Ser, cell line AG28269N and KO cell line	31
17	IF images of control cell line AG28269B stained for DAPI, N cadherin and <i>FOXG1</i> .	32
18	IF images of <i>FOXG1</i> knockout line for DAPI, N cadherin and <i>FOXG1</i>	33

LIST OF TABLES

Table No.	Table Name	Page No.
1	List of disorders that cortical organoid research has been done on	5-6

ACKNOWLEDGEMENTS

I would like to express my sincere gratitude to Alysson R. Muotri for granting me the opportunity to join his laboratory. I consider myself extremely fortunate to have the privilege of working under his guidance. He is a very encouraging mentor who motivated me throughout my journey as a researcher in his lab. Thank you, Alysson Muotri, for your unwavering support.

I am also deeply grateful to Angels Almenar and Thiago Turaca for taking me under their wing and allowing me to contribute to such a novel and ambitious project under their guidance. Angel's daily mentorship has played a pivotal role in shaping me into the scientist I am today and making me realize my potential. I am truly grateful for their mentorship and would like to express my sincere thanks for their guidance, patience, and unwavering support.

I would also like to extend my heartfelt appreciation to Adam Engler and Brian Aguado for generously dedicating their time and effort as members of my committee. Their encouragement and support were invaluable in guiding me to this point in my research journey.

ABSTRACT OF THE THESIS

Modeling *FOXG1* Syndrome: Enhancing model Accuracy and Biomimicry

by

Sneha Iyer

Master of Science in Bioengineering

University of California San Diego, 2023

Professor Alysson Muotri, Chair

Professor Adam Engler, Co-Chair

Disease modeling for neurodevelopmental disorders has long been a challenging endeavor, necessitating innovative approaches to understand the underlying mechanisms. Traditional animal models, while informative, often fail to fully capture the intricacies of human brain development and associated diseases. *FOXG1* syndrome, caused by mutations in the Forkhead box protein G1 (*FOXG1*) gene and characterized by forebrain developmental abnormalities, represents one such

disorder with a range of neurological symptoms including motor deficits, intellectual retardation, and seizures. In recent years, cortical brain organoid models derived from human pluripotent stem cells have emerged as a revolutionary tool in neuroscience research, providing a three-dimensional representation of the human brain. These organoids exhibit structural and functional resemblance to developing brains, encompassing the formation of diverse cell types and the establishment of functional networks. In this study, we were successfully able to develop a cortical organoid model using both healthy and patient derived cell lines for investigating *FOXG1* syndrome, with the patient lines accurately reproducing the microcephaly phenotype observed in FOXG1 syndrome. We explored strategies to enhance the cortical identity of the model using Wingless/Integrated pathway (WNT pathway) inhibition, achieving promising results. Furthermore, we successfully recapitulated neural tube development by constructing a single rosette organoid, thereby increasing its biomimetic properties. Our findings highlight the potential of cortical organoids as powerful tools for studying human neurodevelopment and neurodevelopmental disorders, offering new avenues for understanding disease pathogenesis and facilitating the development of targeted therapeutic interventions.

CHAPTER - 1

Introduction

FOXG1 Syndrome

FOXG1 protein belongs to a family of transcription factors known as forkhead box proteins (FOX). These proteins have been shown to play a very crucial role in neurodevelopment and the maturation of the nervous system, starting from neurogenesis to the patterning of the forebrain (1). It is essential for the proper function and formation of the forebrain and is predominantly expressed there.

Mutations in the gene can lead to aberrations in the forebrain development, potentially resulting in a wide range of neurological symptoms like motor deficits, intellectual retardation, seizures etc. (2). They can also manifest as respiratory and gastrointestinal problems. This is the cause of the rare genetic syndrome called the FOXG-1 syndrome. The syndrome is characterized by severe developmental delays, intellectual disability, and movement disorders, among other symptoms. Despite the rarity of the condition, the study of *FOXG1* Syndrome is of great importance as it sheds light on the fundamental mechanisms underlying brain development and function.

As of January 2023, there have been 1000 reported cases of *FOXG1* syndrome worldwide, and the number of diagnosed individuals is on the rise due to the increasing availability of genetic testing. (3). So far, mutations like deletions, duplications, frameshifts and point mutations have been identified to be associated with *FOXG1* syndrome (3). Dysregulation of *FOXG1* expression exerts profound effects on brain development, while complete loss of the gene can lead to neonatal mortality (4).

Current models to study *FOXGI* Syndrome:

Animal models, such as transgenic mice with targeted *FOXGI* gene mutations, have been instrumental in understanding the molecular and physiological functions of *FOXGI*(5). These models have provided valuable insights into the developmental abnormalities, synaptic dysfunctions, and altered neuronal circuitry associated with the syndrome. *FOXGI* knockout mice models have been developed using lacZ, Tet or Cre genetic engineering systems (6). They all exhibited severe microcephaly and mortality at birth (7). However, haplo-insufficient *FOXGI*Cre/+ mice survived and showed altered neurogenesis phenotypes in the hippocampus and cerebral cortex, epileptic seizures (5). They also exhibited agenesis of the corpus callosum (6).

Although mice models have yielded valuable insights into the pathophysiology of neurodevelopmental disorders in general, they are not always sufficient for understanding human-specific brain development and diseases. They do not accurately represent human brain development and function as there are significant differences between human and mice brains in terms of structure, development, and function and genes. This means that findings from animal studies may not always be applicable to humans.

They also don't fully capture the range of symptoms seen in humans with *FOXGI* syndrome, which can make it difficult to study the disorder in a meaningful way. They are not able to fully recapitulate the genetic changes that cause *FOXGI* syndrome. Animal models of the disorder involve altering the mouse homolog of the *FOXGI* gene, which may not fully reflect the genetic

changes that occur in humans. It is also difficult to test potential treatments in mice models as the translation to humans can be challenging. This is because the underlying mechanisms of *FOXG1* syndrome may differ between humans and animal models, and there may be differences in drug metabolism and toxicity between species.

In recent years, the development of human-based models has allowed for more accurate and personalized studies of neurodevelopmental disorders. One such model is induced pluripotent stem cells (iPSCs), which can be generated from skin fibroblasts and can be differentiated into different cell types including neurons and glial cells. The ability to generate patient-specific iPSCs has revolutionized the study of neurodevelopmental disorders by providing a personalized platform for disease modeling and drug discovery. In vitro models utilizing patient-derived iPSCs have facilitated investigations into the cellular and molecular aspects of *FOXG1* syndrome, allowing researchers to study disease-specific features and potential therapeutic targets (2). Another promising approach for modeling neurodevelopmental disorders is the use of brain/neural organoids, which are 3-D structures derived from human pluripotent stem cells that mimic the development of the human brain in vitro. These organoids can recapitulate the formation of various brain regions and cell types, providing a more comprehensive platform for studying the pathophysiology of neurodevelopmental disorders.

Cortical organoids and disease modeling

In recent years, the development of cortical brain organoid models has revolutionized the field of neuroscience by providing a three-dimensional (3-D) model of the human brain. These organoids,

which are derived from human pluripotent stem cells, recapitulate the structure and function of the developing brain, including the formation of various cell types and the establishment of functional networks (8). They have been instrumental in research in genetic neurological disorders, cancers, infectious diseases and regenerative medicine (9). Yoshiki Sasai's group were the first to show that pluripotent cells when grown in 3-D-culture can recapitulate in-vivo organ growth and development (10). They pioneered the concept of self-organizing organoids from mouse and human embryonic stem cells for different regions of the brain, ranging from forebrain to the ventral telencephalon and pituitary gland (11)

Organoids have significant advantages over other disease models- including but not limited to being less expensive, requiring less time and offering a high success rate. They are being extensively used for personalized medicine and drug screening as they can be tested for multiple drugs effectively (12). They can also be combined with CRISPR-Cas9 and other gene editing systems to study genetic disorders and tumor gene mutation (13).

Over the last 10 years, researchers have exploited the ability of organoids to recapitulate physiological processes existing only in humans. This has been very beneficial in the field of disease modeling and has been used to model a number of disorders. tumor organoids are being successfully used in cancer research, such as breast cancer, gastric cancer, pancreatic and thyroid cancer among others (Table 1). They have been shown to be closely similar to original tumors in terms of physical structure, genetic specificity, metabolic activity and metastatic potential (14). They have also led to the development of therapeutics e.g., Wang et al. developed an organoid model for Non-Small Cell Lung Cancer (NSCLC) carrying a mutation in the human epidermal growth factor 2 receptor (HER2). Drug screening performed on these organoids revealed that Pirotinib exhibited a more pronounced inhibitory effect on organoid proliferation compared to

afatinib in vitro experiments (15). Encouragingly, the findings from the subsequent clinical trials aligned with the drug screening results obtained from the organoids, demonstrating the favorable efficacy of Pirotinib (15). Neural (brain) organoids, representing different regions of the human brain hold tremendous promise as a tool for studying the pathophysiology of neurological disorders.

Table 1: Examples of disorders that cortical organoid research has been done on and paved the way for potential therapeutics.

Disease	Potential Therapeutic Advancements	Reference
Autism Spectrum Disorder	Identification of genetic and molecular abnormalities, testing potential drugs for amelioration of symptoms	(16)
Alzheimer's Disease	Study of amyloid-beta plaques and neurofibrillary tangles, identification of therapeutic targets and testing of drugs	(17)
Parkinson's Disease	Modeling dopaminergic neuron degeneration, testing potential drugs for neuroprotection and disease modification	(18)
Schizophrenia	Investigation of neurodevelopmental abnormalities, identification of potential drug targets, and testing of therapeutic interventions	(19)
Zika Virus Infection	Study of viral effects on neural development, identification of mechanisms of infection and potential antiviral treatments	(20)
Rett Syndrome	Modeling MeCP2 gene mutations, studying neuronal maturation defects, exploring potential gene therapy approaches	(21)
Down Syndrome	Investigation of developmental abnormalities, identification of potential therapeutic targets for cognitive deficits	(22)

As mentioned above, cortical organoid can be generated from patient derived skin fibroblasts, which are reprogrammed to Induced pluripotent stem cell (iPSC) (Figure 1). Fibroblasts, which

are commonly found in connective tissues, can be reprogrammed into iPSCs by introducing specific transcription factors, such as Oct4, Sox2, Klf4, and c-Myc. This discovery was made by Yamanaka in 2008 and this reprogramming process resets the cellular identity of fibroblasts, transforming them into a pluripotent state similar to embryonic stem cells. The iPSCs derived from fibroblasts possess the remarkable ability to differentiate into various cell types of the body, including neurons, cardiomyocytes, and hepatocytes, among others. For making cortical organoids they are exposed to specific culture conditions that promote neural induction by providing signaling factors to guide the differentiation of the iPSCs towards neural lineages. The neural progenitor cells (NPCs) derived from the Embryoid Bodies (EBs) are further exposed to signaling molecules and growth factors that promote cortical specification. These factors include fibroblast growth factor (FGF) and Epidermal Growth factor (EGF). The aim is to drive the differentiation of neural progenitors into cortical neural progenitor cells. The cortical neural progenitor cells are then allowed to self-organize and undergo further maturation. Over time, they form distinct cortical structures, including layers and cell types similar to those found in the developing human brain. Throughout the process, we carefully monitor the growth and development of the cortical organoids, providing appropriate culture conditions, nutrients, and growth factors as needed. These steps help guide the iPSCs to differentiate into cortical-like structures, allowing for the study of human brain development and disease.

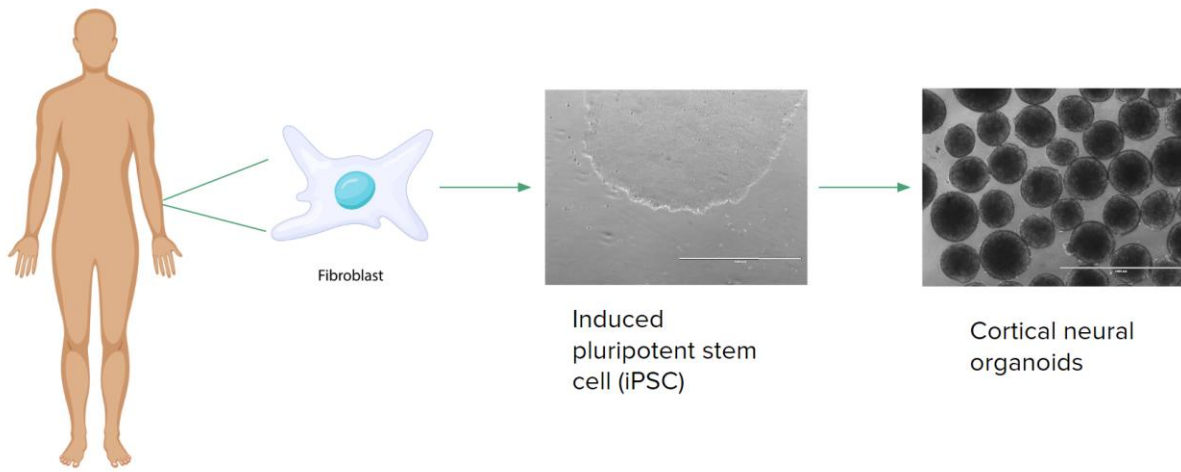


Figure 1: Workflow diagram showing the process of making cortical neural organoids from patient fibroblasts. Scale bar = 1000 μ m

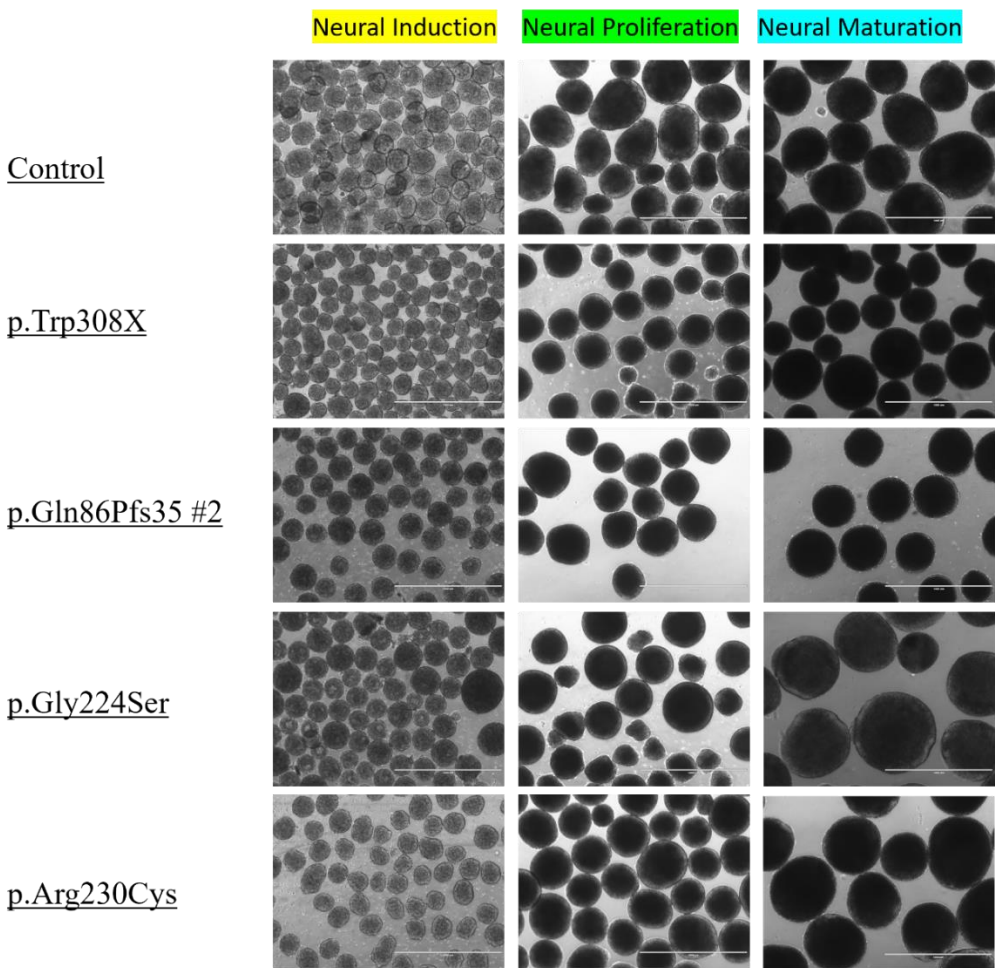
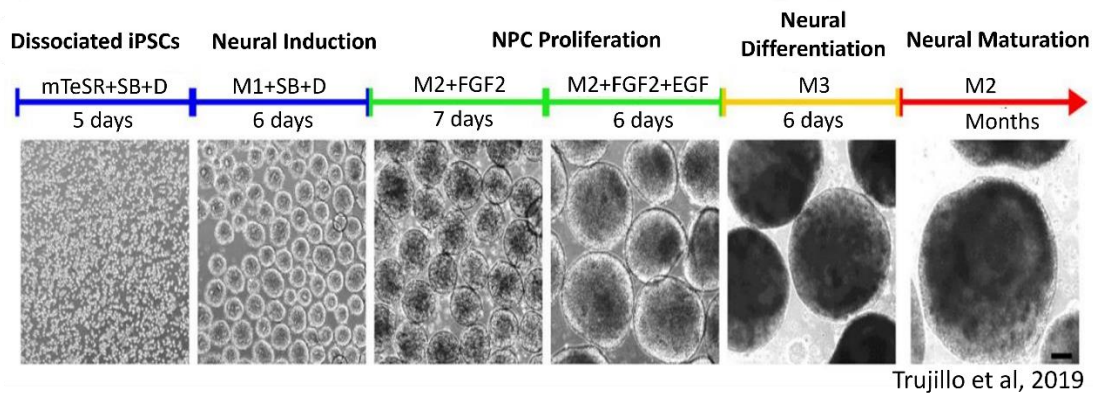


Figure 2: Different stages of depicting cortical organoid generation and growth and the media used. Pictures of control organoids as well as 4 mutant lines taken at different stages of organoid growth. Scale bar = 1000µm

Results:

Generation of *FOXG1* cortical organoids

We were successfully able to generate cortical organoids using the protocol described by Trujillo et al. (8) from already established iPSCs in the laboratory and promote cortical specification which includes 4 stages – Neural induction, NPC Proliferation, Neural differentiation, and neural maturation. Figure 2 shows the different media and factors used in each stage to obtain organoids. To confirm if we were able to generate accurate cortical organoid models for *FOXG1* syndrome, we collected them on day 15, extracted the RNA and performed quantitative Polymerase Chain Reaction (qPCR) to check for expression of *FOXG1*. This would help us to see if *FOXG1* mutant organoids are producing a lower amount of *FOXG1* mRNA as compared to the control organoids due to the presence of mutation in the gene. Reassuringly, we saw that *FOXG1* mutant organoids express lower levels of *FOXG1* mRNA as compared to control organoids (Figure 4). They also produce a lower amount of *LHX2* mRNA, which is another forebrain marker, indicating that *FOXG1* syndrome organoids might not be ‘cortical enough’.

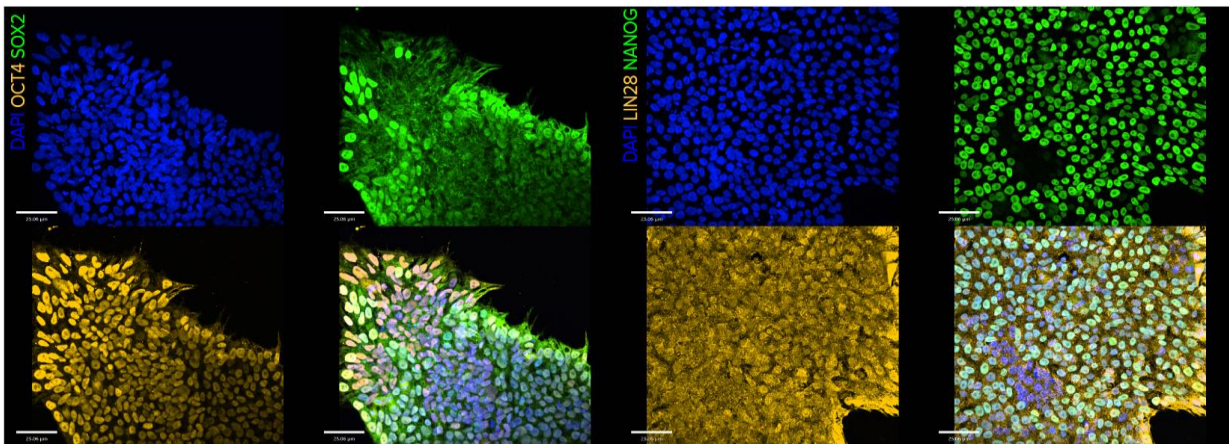


Figure 3: Characterization of p.Gly169Glyfs*23 iPSC Cells. Immunostaining showing the pluripotency markers OCT4, SOX2, NANOG and LIN28. Scale bar = 25.06 μ m

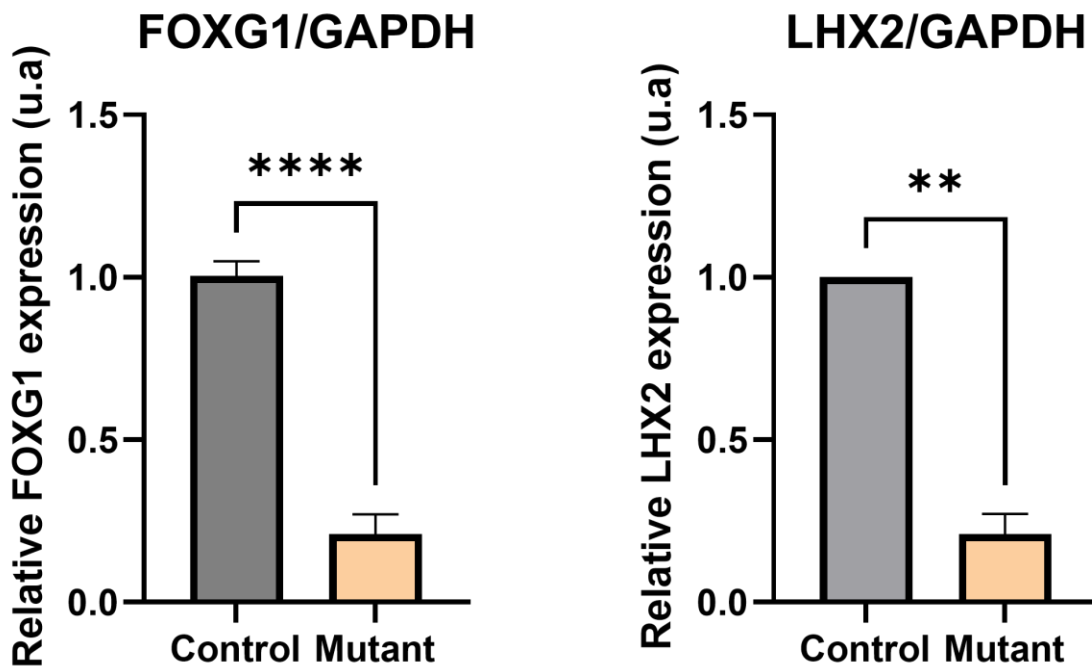


Figure 4: *FOXG1* mutant organoids have lower expression of *FOXG1* as compared to the control organoids. Relative expression of a) *FOXG1* and b) *LHX2* in 15-day old Control and *FOXG1* mutant patient derived organoids normalized to housekeeping gene GAPDH. . N = 5 different patient lines, 1 control with 3 replicates each for *FOXG1*. N = 3 patient lines, 1 control with 3 replicates each for *LHX2*. Unpaired t-test statistical test was performed with alpha value of 0.05

FOXG1 mutant organoids are smaller in size as compared to control organoids.

We took pictures of organoids at each of the different stages (Neural induction, NPC proliferation and Neural Maturation) using EVOS and measured their diameter using ImageJ. We noted that *FOXG1* mutant organoids were significantly smaller in size as compared to control organoids (Figure 5). This observation holds particular intrigue due to its alignment with the microcephaly phenotype frequently observed in individuals with *FOXG1* Syndrome. Our study unveiled a parallel trend within the *FOXG1* cortical organoids, suggesting the potential capacity of these organoids to emulate a cardinal trait of *FOXG1* syndrome, namely its microcephalic manifestation.

Neural Maturation

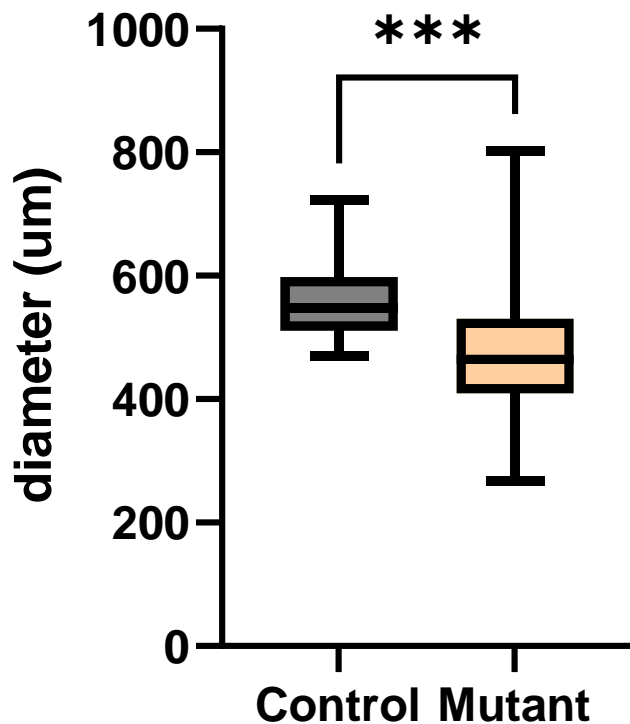


Figure 5: *FOXG1* mutant organoids are smaller than control organoids. Box plot showing the difference in sizes between control and mutant organoids at the neural maturation stage. N = 6 mutant lines. Organoid sizes were calculated based on 2 pictures per cell line and 5 organoids per picture. Unpaired t-test statistical test was performed with alpha value of 0.05

FOXG1 mutant organoids have lower amount of *FOXG1*+ cells

It was observed that mutant *FOXG1* organoids showed a reduced *FOXG1* expression compared to the control organoids. However, a critical distinction remained unresolved: whether this reduction in *FOXG1* expression arises from a diminished production of *FOXG1* within individual cells, or if there is a lower count of cells actively engaged in generating *FOXG1*. Further clarification was

required to discern the precise mechanism underlying the observed decrease in *FOXG1* levels within the mutant organoids. Hence to understand that immunostaining procedure was performed on the organoids to visualize the expression of *FOXG1*. The results of the immunostaining revealed that the mutant organoids indeed contained a lower quantity of cells producing *FOXG1*, as compared to the control organoids. (Figures 6 and 7).

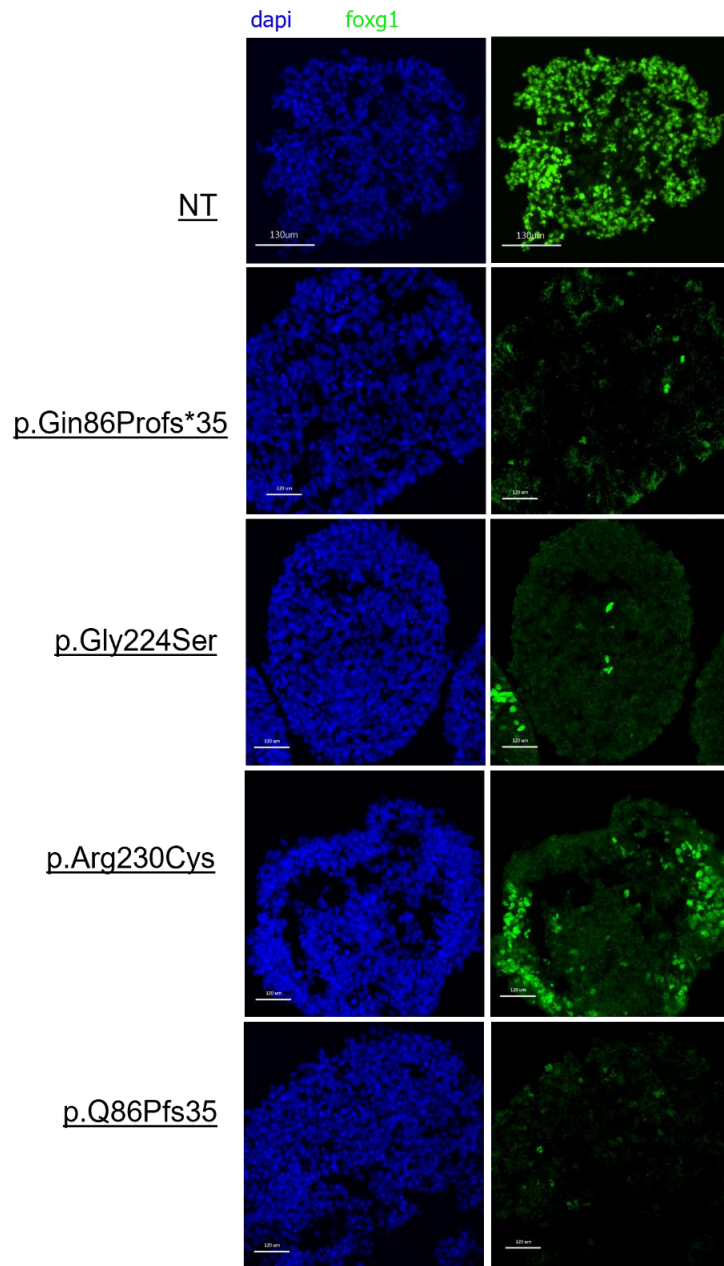


Figure 6: Immunostaining of 15-day old cortical Control and 4 *FOXG1* mutant organoids showing all cells (DAPI) and *FOXG1* positive cells. Scale bar = 120 μ m

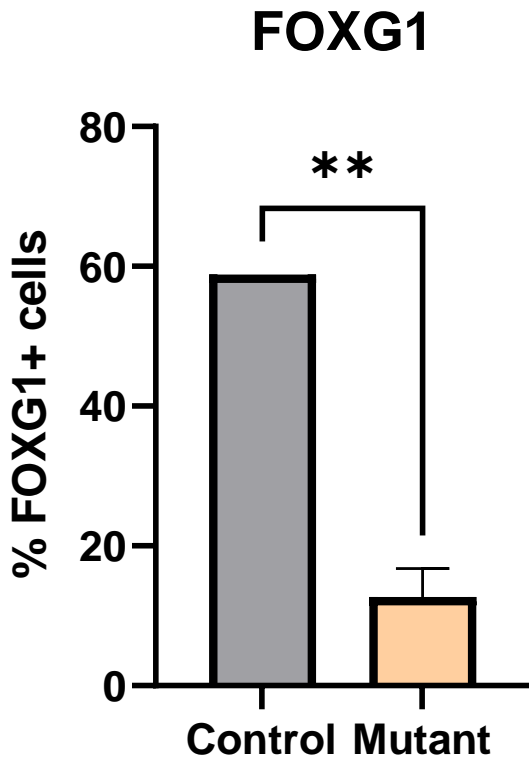


Figure 7: Bar graph showing percentage of *FOXG1* positive cells in Control and *FOXG1* mutant organoids (15 days old). N = 4 different mutant lines (p.Gin86Pfs*35 #1, p.Gly224Ser, p.Arg230Cys, p.Gin86Pfs35 #2). Data was obtained from two organoids per experimental group, each containing four regions of interest (ROIs). All organoids are from a single prep. Unpaired t-test statistical test was performed with alpha value of 0.05

Conclusion/ Discussion

Our study encompassed the successful generation of cortical organoids using *FOXG1* patient derived cell lines. Due to the presence of mutation in the *FOXG1* gene in patients, our anticipations centered on discerning variations in the transcriptional output of *FOXG1*. As anticipated, our experimental outcomes confirmed a significant reduction in *FOXG1* transcript levels in the

FOXG1 mutant organoids, as corroborated by quantitative PCR (qPCR) analysis in comparison to the control organoids. We also saw a significant reduction in the size of mutant organoids, recapitulating the microcephaly phenotype of *FOXG1* syndrome. Furthermore, we also evaluated the cellular manifestation of *FOXG1* by applying immunofluorescence, which unveiled a reduction in the prevalence of *FOXG1* positive cells within the mutant organoids as compared to the control organoids. This dual approach of transcript quantification and protein visualization collectively underscores the perturbed *FOXG1* dynamics in the context of the *FOXG1* syndrome organoids, helping us in better comprehending the implications of *FOXG1* mutation.

In our investigation, the expected decrease in *FOXG1* mRNA in mutant organoids was confirmed, along with a significant reduction in *FOXG1*-positive cell numbers. Notably, a considerable proportion of cells, particularly in mutant organoids, showed no *FOXG1* expression—a trend shared by both control and mutant groups, albeit more prominent in the latter. As our study revolved around cortical organoids, the presumption was for a complete *FOXG1*-positive cell population, given its role as a forebrain marker. While lower *FOXG1* signal intensity was predicted in mutants, the presence of non-*FOXG1*-expressing cells prompts a vital query.

This prompts us to question the extent of cortical maturity achieved in our organoid models. The combination of variable *FOXG1*-positive cells and incomplete cortical features highlights the complexity of the model system, urging further exploration to enhance its accuracy in replicating cortical developmental dynamics.

This raises the question whether our cortical organoid models are “cortical enough” or not.

We also see a ‘multiple rosette’ morphology – which are epicenters of neural progenitor cells organized in a radial pattern, mimicking the early stages of neuroepithelial development in the developing brain (Figure 8). This is analogous to the developing neural tube during early embryonic brain development. We know that the human brain develops from a single neural tube and multiple rosettes are a morphology of neural tube defects/ aberrations. Hence, our organoid model might not be perfect and need some improvements for better biomimicry. See chapter 3.

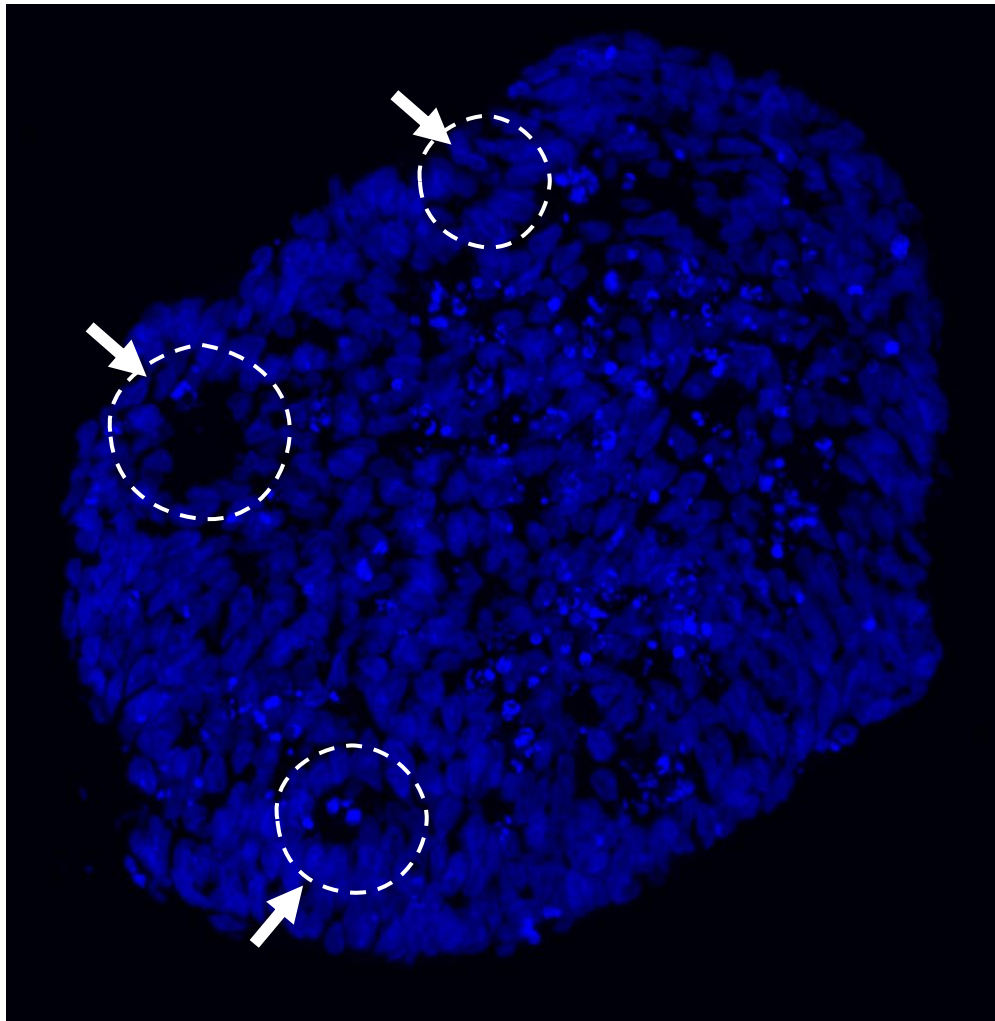


Figure 8: Cortical organoid with multiple rosettes - epicenters of neural progenitor cells organized in a radial pattern, mimicking the early stages of neuroepithelial development in the developing brain.

CHAPTER 2

WNT inhibition to improve cortical identity

As mentioned above, we followed the cortical organoid generation protocol specified by Trujillo et al. Herein we use dual SMAD inhibition to derive the iPSCs to cortical fate, which refers to the generation and differentiation of cells that give rise to the cerebral cortex, the outer layer of the brain responsible for higher cognitive functions. During the early stages of brain development, pluripotent stem cells undergo a process called neural induction, where they are directed to differentiate into neural progenitor cells. These neural progenitor cells subsequently give rise to specific cell types within the brain, including cortical neurons. Dual SMAD inhibition is employed to promote the specification of neural progenitor cells toward cortical fates. By blocking the activity of SMAD2 and SMAD3 proteins, which are involved in the TGF- β signaling pathway, the inhibitory signals that could otherwise divert the fate of neural progenitor cells away from cortical development are attenuated. This leads to a reduction in the signaling activity of TGF- β , which allows for the activation of other signaling pathways that promote cortical specification. This inhibition creates an environment conducive to the generation of cortical neurons and suppresses alternative differentiation pathways that may lead to the formation of non-cortical cell types.

Researchers have used various cortical organoid fate generating protocols over the years, ranging from dual SMAD-I, inhibitor free conditions, TGF- β and WNT inhibition and combined dual SMAD-I and WNT-I (triple inhibition) (23).

Using and comparing bulk and single cell RNA-Seq data of organoids derived using various directed derivation methods, it has been shown that a brief and early exposure to WNT inhibition

along with dual SMAD inhibition enhances cortical Neural Stem Cell (NSC) identity while suppressing non-cortical fates at the same time. (23) This also enables the formation of well-defined cortical germinal zones, making them suitable for modeling microcephaly (23), which could be useful for modeling *FOXG1* where we see microcephaly as a phenotype.

Coming back to the findings highlighted in Chapter 1 through our Immunofluorescence analysis, the intriguing presence of a subset of cells devoid of *FOXG1* signal offers a valuable insight. This observation raises the plausible conjecture that our cortical organoids might not achieve full forebrain differentiation, considering *FOXG1*'s pivotal role as a forebrain marker. Hence based on the studies mentioned above, we hypothesize that we'd be able to optimize our cortical organoid model using a commonly used WNT inhibitor XAV-939 along with TGFB and BMP inhibitors SB-431542 and Dorsomorphin. (23)

In order to check if our hypothesis is true we'd compare cortical brain marker *FOXG1* levels using both standard and WNT inhibitor protocol. We expect to see an increase in *FOXG1* positive cells (using Immunofluorescence) as well as *FOXG1* levels (using qPCR) in both neurotypical and *FOXG1* mutant organoids.

Results

WNTi increases the number of *FOXG1*-expressing cells in *FOXG1* mutant organoids.

In the context of our study, we performed immunostaining on 15-day-old control and mutant organoid samples, employing *FOXG1* and neuronal markers Nestin, KI67, and Sox2 to confirm brain organoid identity. This analysis was conducted under two conditions: with and without the WNT inhibitor XAV-939. Remarkably, XAV-939 treatment resulted in a distinct response pattern.

Notably, mutant lines exhibited an increased *FOXG1*-positive cell population, while the control line displayed a minor (~10%) reduction under the same treatment. (Figures 9 and 10). The qPCR results also show the same trend with XAV-939 treatment increasing the amount of *FOXG1* transcripts for the mutant organoids but not for the NT organoids (Figure 11). Administration of XAV-939 yielded another significant result: an increase in LXH2 mRNA expression, another distinct forebrain marker. This finding suggests a compelling notion that the inhibition of WNT signaling potentially prompts the organoids towards a more defined cortical lineage hence making them more “forebrain-like”.

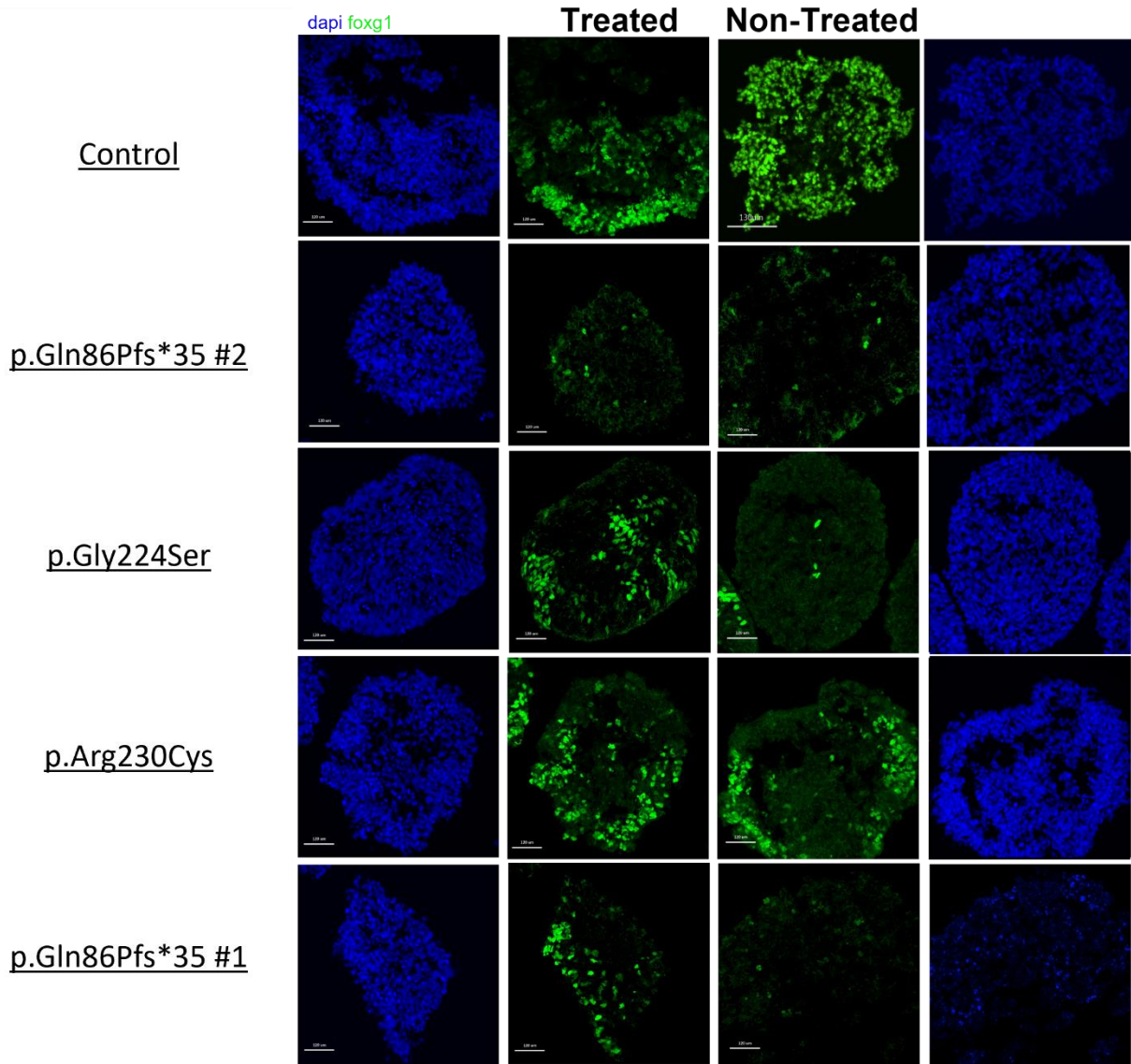


Figure 9: Representative immunostaining images of 15 day old cortical organoids (Control and 4 *FOXG1* mutants) with and without treatment with XAV-939 showing all cells (DAPI), *FOXG1* positive cells. Scale bar = 120 μ m

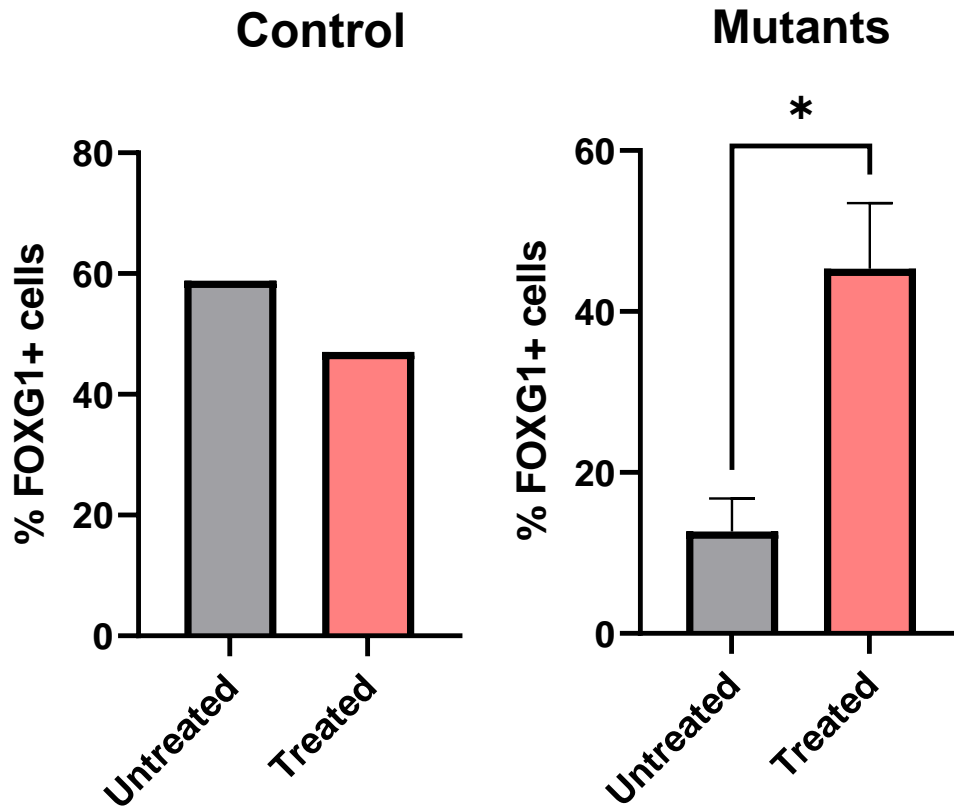


Figure 10: Bar graph showing percentage of *FOXG1* positive cells in control and *FOXG1* mutant organoids (15 days old) with and without treatment with XAV-939. N = 4 different mutant lines (p.Gln86Pfs*35 #1, p.Gly224Ser, p.Arg230Cys, p.Gln86Pfs35 #2). Data was obtained from two organoids per experimental group, each containing four regions of interest (ROIs). All organoids are from a single prep. Unpaired t-test statistical test was performed with alpha value of 0.05

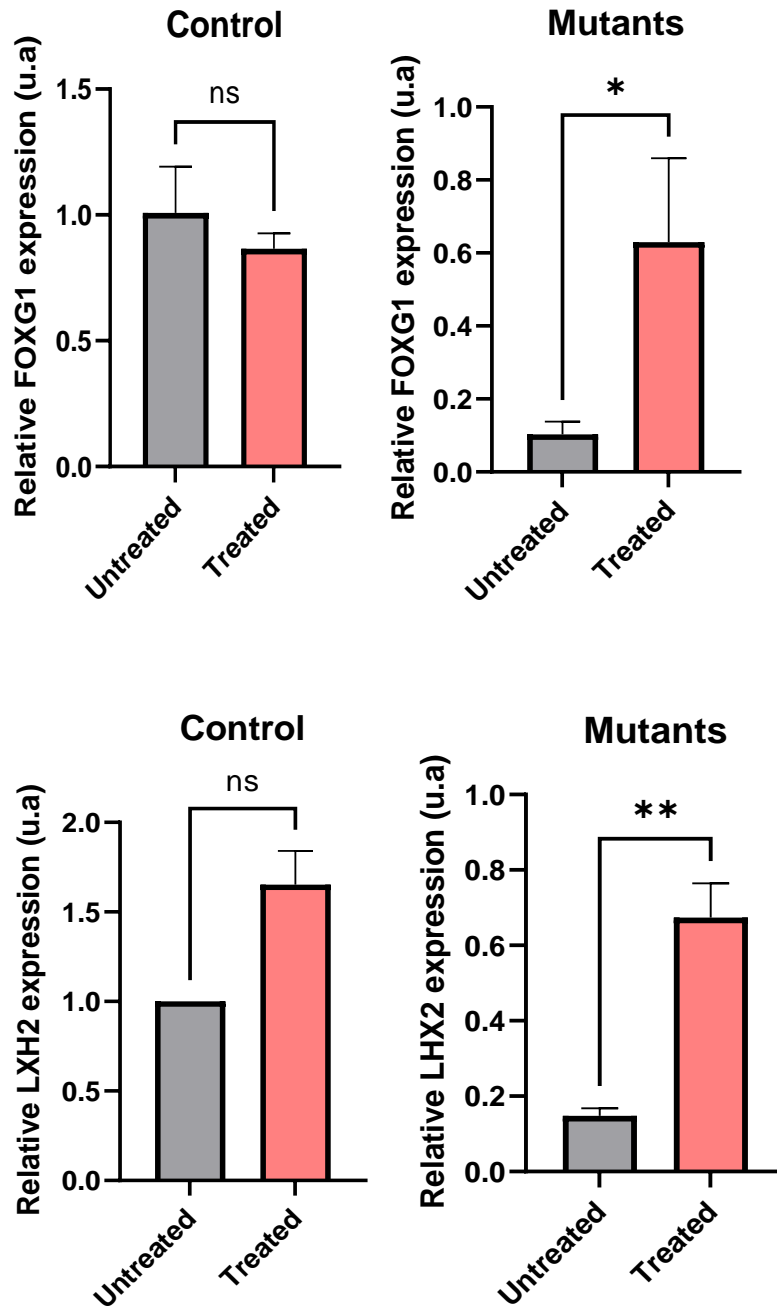


Figure 11: Relative expression (RT-qPCR) of *FOXG1* in 15-day old Control and *FOXG1* mutant patient derived organoids with XAV-939 treatment and Relative expression of another forebrain marker LHX2 with XAV-939 treatment. ~10 organoids collected from one well each per sample from a single prep. Both genes are normalized to GAPDH. Unpaired t-test statistical test was performed with alpha value of 0.05

Conclusion/Discussion

We were able to increase *FOXG1* in mutant organoids by using WNT inhibitor and hence potentially improved our cortical organoid model by deriving it to a more cortical fate. Increase of another forebrain marker *LXH2* also strengthens this possibility of a more accurate, telencephalic organoid. We were also able to increase the number of *FOXG1* positive cells in mutant organoids, however, the increase wasn't significant. Since these results are only from 2 organoids per cell line and from a single prep, further experiments are needed to validate these results with a greater number of replicates. We were still not able to get 100% *FOXG1* positive cells, which is what we expect from cortical organoids (24)

Feeder-dependent iPSC's are maintained with a much lower concentration of FGF2 (4ng/ml) and are successfully able to form forebrain organoids (25) as compared to 20ng/ml what we use in our protocol. Greber et al also showed that FGF2 is crucial for maintaining pluripotency as well as inhibiting neural induction (26). Sato et al were able to show an almost 100% *FOXG1* positive cells population using a much lower FGF2 concentration to make forebrain EBs and 0% *FOXG1* positive cells using a higher FGF2 concentration (25). Hence using a lower FGF2 concentration would be another way to obtain "more cortical" organoids in addition to WNTi treatment. Getting cortical organoids is crucial for establishing accurate models of *FOXG1* and other disorders affecting the forebrain. Many neurological disorders, such as autism, schizophrenia, and epilepsy, are associated with abnormalities in the cortex. Cortical organoids offer a way to model these disorders more accurately than simpler organoids focusing on other brain regions. Additionally, the cerebral cortex is one of the most complex and evolved regions of the brain, responsible for

many higher-order functions such as cognition, perception, and consciousness. Studying cortical development and disorders is crucial due to its significance in human brain function.

CHAPTER - 3

Single rosette organoid model

In vivo, a single neural epithelium tube gives rise to the whole central nervous system. But in vitro organoids are traditionally grown from multiple rosettes - which are flower-like epicenters giving rise to the neural tube (Figure 9). Organoids arising from multiple rosettes have been shown to have an unpredictable organization and structural heterogeneity (27). The presence of multiple rosettes is also a phenotype of abnormalities at birth such as diastematomyelia and diplomyelia (28)- which don't make them ideal for modeling healthy neuronal development and disease. Therefore, in order to make our cortical organoids more biomimetic, it's important to generate organoids arising from a single rosette. Moreover, most cells in cortical organoids generated from a single rosette have been shown to express FOXG1 (29), making them ideal for modeling forebrain development and disorders.

There are 2 main ways of generating single rosette organoids - using a micropattern substrate or manually isolating the rosettes. In the manual isolation methods, single neural rosettes are manually scraped off, plated into another dish and allowed to grow into an organoid consisting of just one rosette (29). This method is one of the most reliable methods of generating critical biomimetic cytoarchitecture within organotypic Central Nervous System tissues (CNS) tissues (30). However, it is a cumbersome and a very technical process which requires a lot of time, given the percentage of recovery is also not 100%.

Recent studies have demonstrated that by subjecting hPSC tissues to geometric confinement on 2-D micropatterned substrates, it is possible to induce self-organized embryonic patterning (31). This

process closely resembles gastrulation and is dependent on the specific morphology of the confined tissues. This model also helps us visualize neural tube formation, which is the earliest and a very crucial step to forebrain patterning. Hence, we decided to use this method to generate a single rosette organoid and see if we can use this to model *FOXG1* syndrome. This would allow us to see if *FOXG1* causes any changes to the neural tube morphology at the neurulation stage itself, which conventional cortical organoids fail to replicate.

We used micropattern plates of 500 μm diameters for iPSCs to grow on and followed the protocol by Karzbrun et al to generate an organoid recapitulating neural tube formation (32). The selection of the 500 μm micropattern size was motivated by its proximity to the 450 μm dimension. Notably, previous experiments utilizing 450 μm micropatterns revealed neural epithelial dimensions of $216 \pm 11 \mu\text{m}$ in width and $66 \pm 7 \mu\text{m}$ in thickness. These dimensions closely mirrored those observed in the human neural plate during Carnegie stage 8 (32). The organoids were also cleared before imaging as clearing thick tissue samples before imaging improves image clarity, depth, and signal-to-noise ratio by reducing light scattering and allows for better visualization of 3D structures. Protocol described in detail in materials and methods (33).

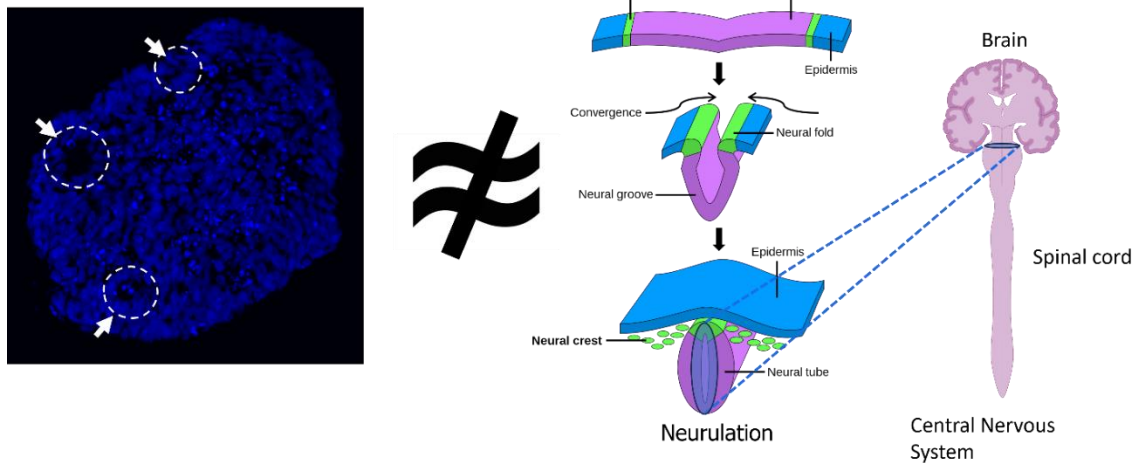


Figure 12: Schematic showing how the presence of multiple rosettes in organoids do not accurately recapitulate human neural tube formation and development.

Results:

Single rosette organoid generation

We used micropattern dishes from 4D cell technology which had patterns measuring 500uM each (Figure 13). We coated the plates with 1.6% Matrigel and seeded 1M iPSCs onto the plate. The protocol was followed as described by Karzbrun et al (Figure 14) (also described in Materials and Methods) (32).

We fixed the organoids on day 10 and performed immunofluorescence on them and stained them for *FOXP1*, *SOX2* and N-cadherin. *SOX2* is a marker for neural progenitor cells and is one of the markers to confirm cortical brain organoid identity. N cadherin stains the apical side of neuroepithelial cells and helps to visualize the inside of the “rosette” (32). We saw that one of the Control lines (WT83c6) had a hollow center with no cells, indicating the possibility of a neural

tube -like structure (Figure 15). However, the N-cadherin which is supposed to stain the inner apical membrane of the neuroepithelium wasn't exclusively limited to the center of the organoid around the hollow structure (Figure 15). We used another Control line (AG28269B) to see if we can replicate the results for a different control line and it seems to have worked better with a single rosette and a lot of N-cadherin inside the 'rosette' for both the replicates (Figures 16 and 17). We also used a *FOXG1* mutant Gly224Ser which seems to have 2 rosettes (Figure 16) and *FOXG1* KO seems to have an interesting morphology with a lot of N-cadherin in between the cells (marked with DAPI) (Figure 17). *FOXG1* KO served to act as a negative control for the *FOXG1* antibody. AG control line and mutant lines are positive for *FOXG1*, and the KO line isn't, which is expected. The KO line also serves as a negative control for our *FOXG1* staining, hence it confirms if what we're seeing in other cell lines is actually *FOXG1* or just background/ noise/non-specific staining. This result is particularly intriguing as it unveils the presence of *FOXG1* during an early neurodevelopmental stage, a revelation hitherto unreported. While *FOXG1* is recognized for its involvement in neurogenesis, typically commencing at approximately 5 weeks of gestation, our findings demonstrate its presence during the neural tube formation phase, a developmental milestone occurring between the 3rd and 4th weeks of gestation (34).

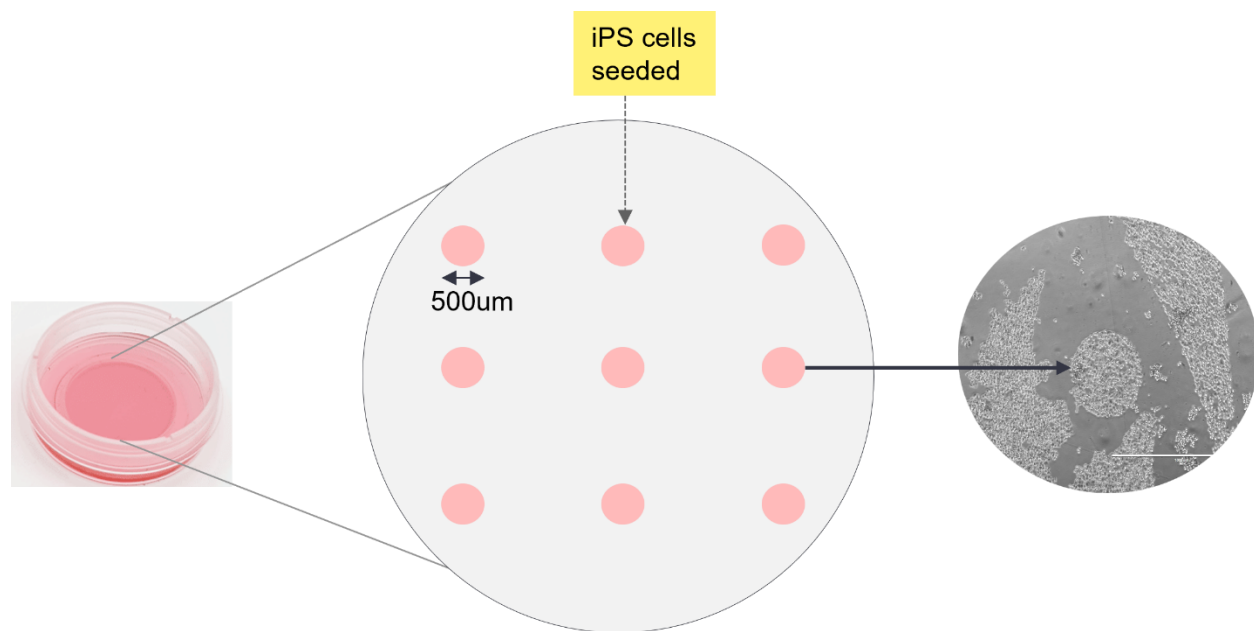


Figure 13: Schematic showing the design of the micropattern dish consisting of a glass bottom with micropatterns of 500 um diameters. iPSCs are seeded onto it.

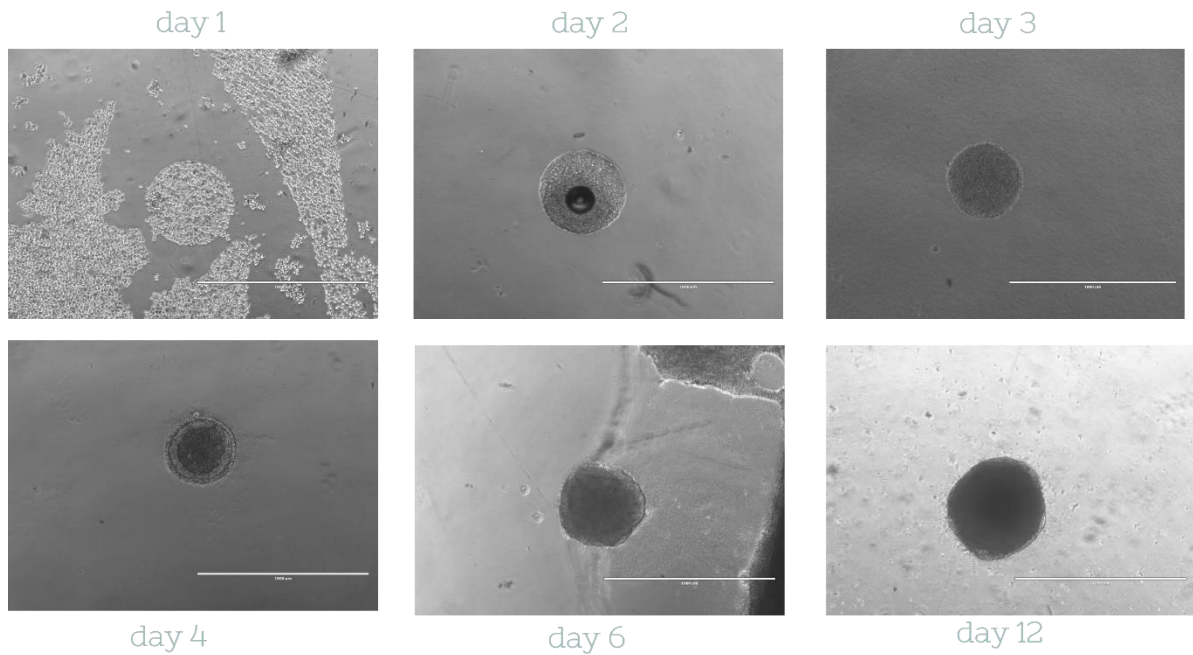


Figure 14: Pictures of organoid development throughout 10 days. Matrigel is added to the media on day 2 to transform the 2-D iPSC colony into 3-D colonies. The cells were exposed to a combination of morphogens believed to play a role in early neural development. Initially, a neural induction medium containing TGF- β inhibitor called SB-431542 was applied, followed by exposure to bone morphogenetic protein 4 (BMP4). As a result, the system displayed self-organized pattern formation and folding morphogenesis. Scale bar = 1000 μ m

sox2 ncadherin

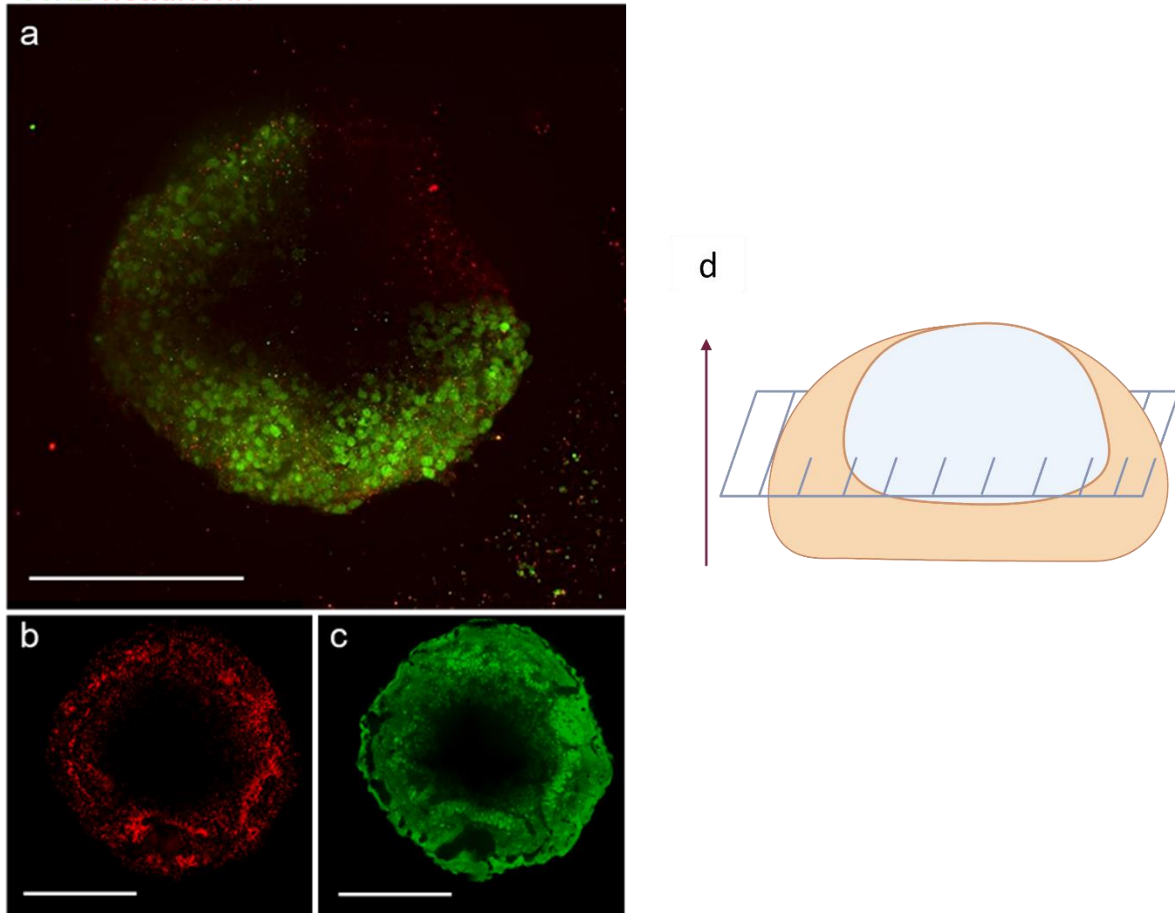


Figure 15: IF images of the middle plane of single rosette organoid from WT83C6 control cell line stained for SOX2 (neural progenitor cell marker) and N-cadherin (neuroepithelium marker). d) diagram of the single rosette organoid structure and the highlighted plane. Scale bar = 250 μ m

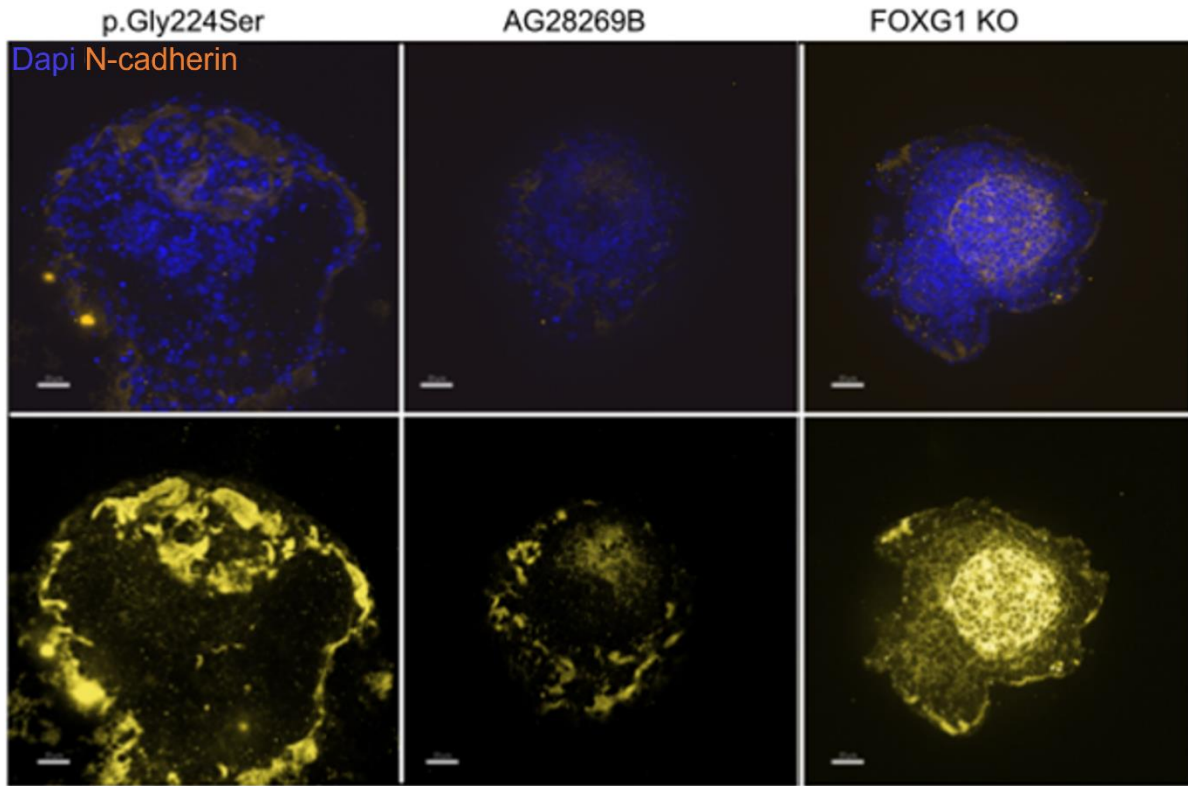


Figure 16: IF images of *FOXG1* mutant cell line p.Gly224Ser, control cell line AG28269N and Knockout cell line stained for DAPI and N-cadherin. Scale = 30 μ m.

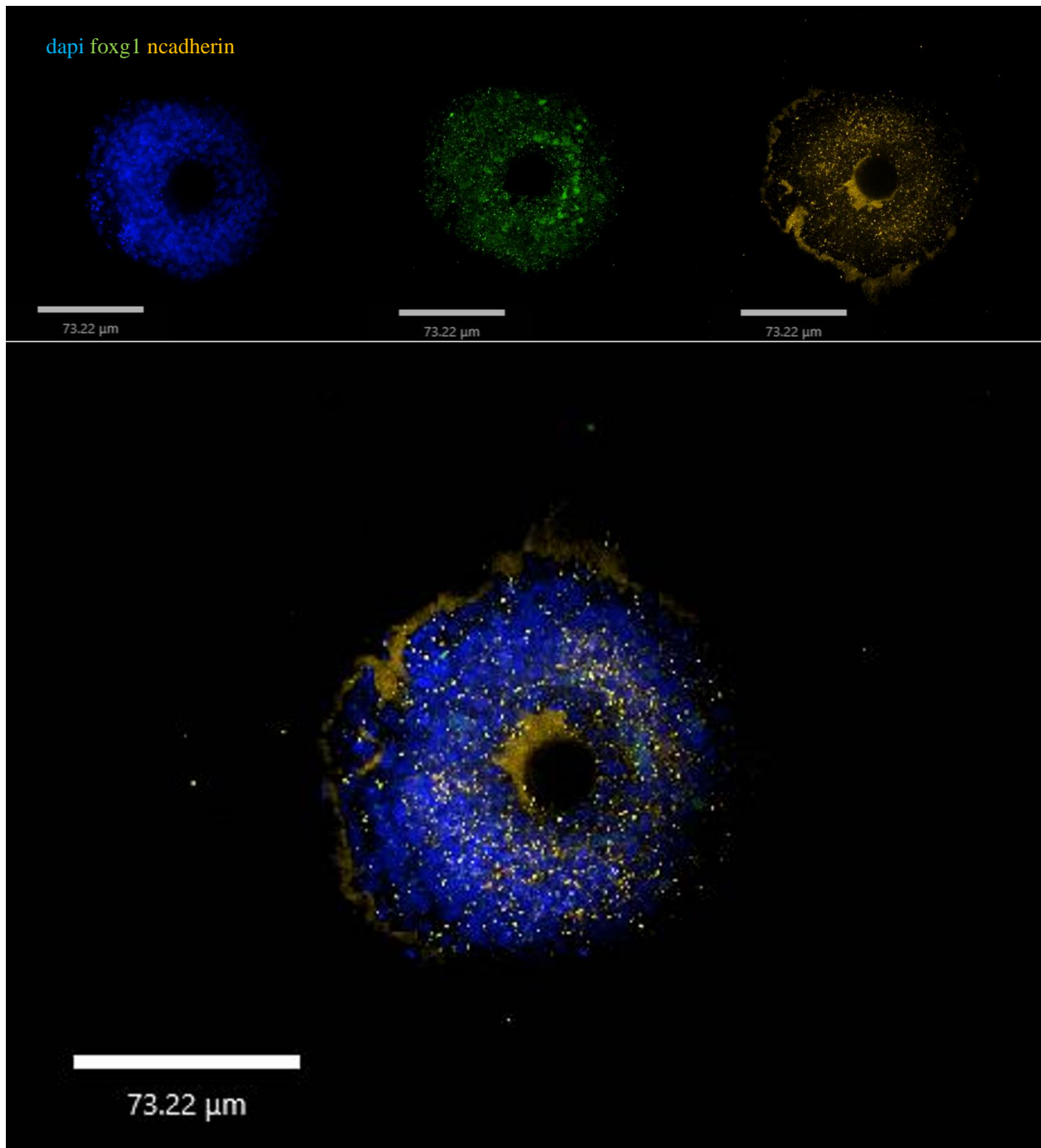


Figure 17: IF images of control cell line AG28269B stained for DAPI, N-cadherin and *FOXG1*. Scale bar = 73.22μm.

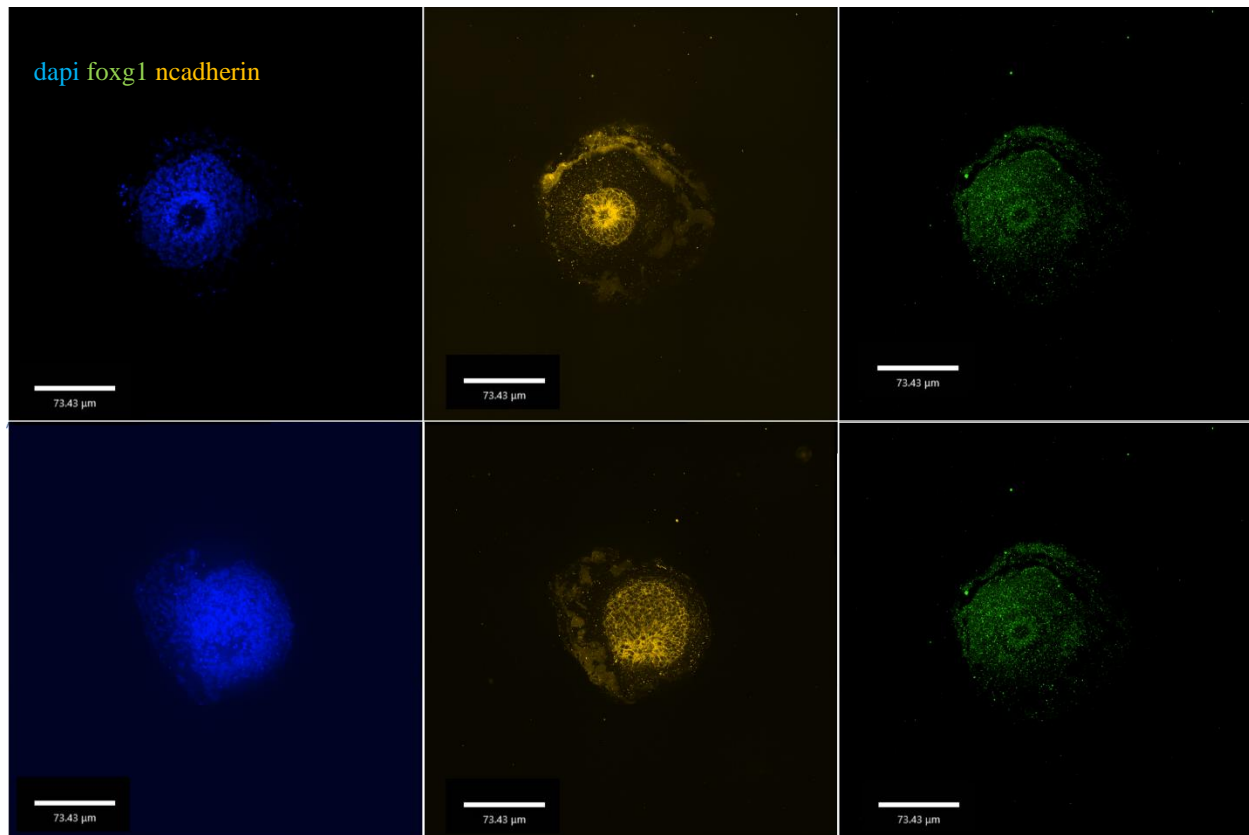


Figure 18: IF images of *FOXG1* knockout line for DAPI, N-cadherin and *FOXG1*. Scale bar = 73.22 μ m.

Conclusion:

We attempted to create a single rosette organoid using geometric restraints and saw positive results. WT83C6 control line has a hollow center, possibly representing a single neural tube with N cadherin around it but more replicates and further experiments need to be done to have more robust results. AG28269B and KO lines worked well and we could see clear single rosette morphology- although *FOXG1* KO line had more intense N-cadherin staining in the center and between the cells. This could be a result of lack of *FOXG1* in the KO lines that gives rise to such a morphology. We were successfully able to form a 3-D organoid as seen through the dome-like structure going through the different layers of the Z-stack (See supplementary videos).

DISCUSSION

We successfully established a proof-of-concept framework for studying *FOXG1* syndrome and other neurological disorders. Moreover, this model can also be utilized for studying neurodevelopmental processes. By employing this model, we aim to gain insights into the underlying mechanisms and potential therapeutic strategies for these conditions. The construction of our model involved the utilization of patient-derived cell lines and *FOXG1* KO line ensuring a personalized and specialized approach to studying *FOXG1* syndrome. This personalized aspect of the model enhances its relevance and applicability to the specific disease of interest.

In order to enhance the cortical identity of our model, we employed an inhibition strategy targeting the WNT pathway (23). The results obtained from this approach demonstrated an increase in the number of *FOXG1* positive cells in the mutant organoids after WNTi treatment. The presence of a higher number of cells producing *FOXG1* implies that the organoids show an enhancement of cortical identity, which indicates the effectiveness of WNT pathway inhibition. However, it is important to note that further improvements can still be made. We did not see an increase in *FOXG1* positive cells for control organoids after treatment. Combining WNT inhibition with other methods, such as reducing the concentration of fibroblast growth factor (FGF), could potentially lead to even greater enhancement of cortical identity (25). Although our model did not achieve 100% *FOXG1* expression, these alternative approaches hold promise for further refinement.

Additionally, we showcased the capacity of organoid-based models to mimic the neural tube formation stage of human brain development. By utilizing hiPSC, we successfully constructed a

single rosette version of the *FOXG1* syndrome organoid model (Gly224Ser) as well as some other cell lines. This achievement provides a valuable platform for studying the early stages of neurodevelopment and gaining a deeper understanding of the pathological processes underlying *FOXG1* syndrome, as it aims to recapitulate one of the earliest stages of human neurodevelopment – formation of the neural tube or neurulation. Our developed model allows for the tracking of phenotypic and cell-type specific changes in gene expression throughout various stages of cortical brain development, commencing as early as the neurulation stage and gives us valuable insight into the role of *FOXG1* at this stage. This capability also provides insights into the dynamic changes occurring during neurodevelopment and aids in elucidating the molecular mechanisms involved in *FOXG1* syndrome and related disorders. The *FOXG1* knockout (KO) model, lacking *FOXG1* expression entirely, functions as a negative control for validating the *FOXG1* antibody. It also offers an opportunity to explore the impacts of *FOXG1* on neurodevelopment through comparisons with *FOXG1* syndrome patient lines, which possess *FOXG1* gene mutations but are not complete knockouts.

Looking ahead, the utilization of cortical organoid models, such as the ones presented in my thesis, holds great potential for guiding the design of therapeutic interventions for neurodevelopmental diseases. In summary, our study successfully constructed specialized models for investigating *FOXG1* syndrome and other neurological disorders, using patient-derived cell lines. Through the inhibition of the WNT pathway, we enhanced the cortical identity of this model by increasing the number of *FOXG1* positive cells in the mutant organoids, although further optimization is required. Additionally, we demonstrated the ability of organoid-based models to mimic neural tube formation, providing a platform for studying early neurodevelopmental stages. Furthermore, the

application of such models in therapy design holds promise for reducing the prevalence and impact of neurodevelopmental diseases.

MATERIALS AND METHODS

***FOXG1* hiPSC Lines and reprogramming:**

FOXG1 patient fibroblasts from 7 different patients were obtained from the explants of dermal biopsies following informed consent under protocols approved by UCSD Institutional Review Board (35).

Cell culture and organoid differentiation

8 different lines of human induced pluripotent stem cells (7 *FOXG1* lines and one control line) were cultured on Matrigel (Corning, insert catalog number) -coated plates and maintained using mTesR Plus (#100-1130, STEMCELL Technologies,) every alternate day.

Neural Induction

iPSCs were grown to confluence and dissociated using a 1:1 mixture of DPBS and StemPro™ Accutase™ Cell Dissociation Reagent (#A1110501, Thermo Fisher Scientific) and transferred to 6-well plates, with each well containing approximately 4M cells and mTesR Plus media, 10μM Rock Inhibitor, 10μM SB (#04-0010, Stemgent) and 1μM Dorsomorphin (#3093, R&D Systems). They were then maintained in suspension at 37°C on a 95-rpm shaker. After 2 days, Neural Induction media (M1) was used instead of mTesr plus, for 6 days and changing media everyday. M1 media was prepared using DMEM/F12 (Life Technologies, 10565042), 1% Glutamax (Life Technologies, 35050061), 1% N2 Neuroplex (Gemini, 400163 005ML), 1% non-essential amino

acids (Gibco, 11140-050), 1% Pen-Strep (Life Technologies, 15140163), 1 μ M of Dorsomorphin (Tocris, 309310), and 10 μ M SB-431542 (SB, Stemgent, 04-0010-10).

NPC proliferation

On day 9, mtser plus media is replaced by NPC proliferation, M2F, consisting of Neurobasal media (Life Technologies, 21103049), 2% Gem21 Neuroplex (Gemini, 400160010ML), 1% non-essential amino acids, 1% Glutamax and 20 ng/mL Fibroblast Growth Factor bFGF (PeproTech) for 7 days with media changes every day. After that, each well of spheres is split into 2-3 wells and 20 ng/mL Epidermal Growth Factor EGF (PeproTech) is also added in addition to M2 media (M2EF media).

Neuronal Maturation

On the 22nd day, M2 media is supplemented with Neurotrophic factor (BDNF, Peprotech 450-02), glial cell-derived neurotrophic factor (GDNF, Peprotech 450-10), neurotrophic factor 3 (Gemini, NT3, 300-107P), ascorbic acid (Sigma Aldrich, A4403 SIGMA), and dibutyryl-cAMP (Fisher Scientific, 1141/10), replacing FGF2 and EGF for 6 days with media changes everyday. From day 28 onwards, organoids are maintained in M2 media with no factors. Media is changed on day 30 and then after every 3-4 days.

Organoid size measurement:

EVOS FL Imaging system was used to image organoids throughout the neural induction, proliferation and maturation stages with a 4x magnification. ImageJ was used to calculate the diameter of the organoids using the line tool and the graphs were created using Graphpad prism.

Organoid collection

Organoids were collected on day 15 from all the samples by transferring them to Eppendorfs. They were then washed with ice cold PBS and transferred to dry ice and stored at -20C.

RNA extraction and DNase treatment:

QIAGEN RNeasy Mini Kit (Qiagen, 74134) was used to extract RNA from 15day old cortical organoids with subsequent DNA removal using *TURBO DNA free* (catalog number). The extracted RNA was measured using Nanodrop (Thermo Fisher) and Qubit (Company name).

CDNA preparation and target amplification:

RNeasy Plus Mini Kit (# 74134, Qiagen, Germany) is used to extract RNA from all the samples. First strand cDNA synthesis was performed using Oligo(dt). Reverse transcriptase was added to all the samples except for the no RT controls. To amplify target DNA, a master mix was prepared using RT² SYBR Green Fluor qPCR Mastermix (#330513, Qiagen) and primers and added to the wells of a 96 well plate (BioRad). Prepared cDNA was diluted to 1:5 with RNase free water and transferred into their respective wells in triplicates.

Subsequently, an adhesive film was applied on top of the plate, which was then subjected to PCR amplification using the CFX384 Touch Real-Time PCR Detection System (#1855484, Bio-Rad).

Immunofluorescence imaging:

For iPSCs, cells were washed thrice with DPBS for 5 minutes each. Subsequently, cells were fixed in 4% paraformaldehyde (PFA, Electron Microscopy Sciences) diluted in PBS for 20 minutes, followed by three more washes with DPBS for 5 minutes each. To block and permeabilize the cells, they were incubated in a solution of 0.1% Triton X-100 Permeabilizing solution (CoreBio Services, 1610407) and 3% Bovine Serum Albumin Blocking solution (BSA, Gemini Bio-Products, 700-110) for 30 minutes at room temperature. Next, the cells were exposed to the primary antibodies overnight at 4°C, followed by three washes with DPBS for 5 minutes each the next day. The secondary antibody was added and incubated for 2 hours at room temperature, after which the cells were washed three more times with DPBS for 5 minutes each. Cells were then stained with DAPI (1:5,000, VWR International, 80051-386) for 10 minutes. Coverslips (Fisher Scientific, 1255015) were mounted using Gold Antifade Reagent (Life Technologies, P36930).

For organoids, they were first washed with PBS followed by fixation with 4% PFA in a microcentrifuge tube for 4 hours at RT, then washed thrice and were transferred to 30% sucrose (CoreBio, S0389-1KG) in PBS. Two days later after the organoids had sunk to the bottom of the tube, sucrose was aspirated and the remaining organoids were frozen in Optimal Temperature Compound (OCT, VWR, 25608-930) enclosed within a plastic mold (Fisher Scientific, 50465347) and transferred to -80°C freezer.

The OCT blocks containing the organoids were removed from the plastic mold and were then sectioned using a cryostat (Leica, CM3050S) into 20 µM thick slices. The sliced organoids (2 sections per slide) were then mounted onto glass slides, allowed to dry and then stored at -80C.

For staining the organoids, they were outlined with a hydrophobic barrier pen to ensure tissue coverage during staining (Vector Laboratories, H-4000). Staining and mounting of the slides were carried out using the same protocol as mentioned above.

For the micropattern single rosette organoids, they were washed with PBS and then fixed with 4% PFA for 1 hour followed by washing 3x with PBS for 15 minutes and then parafilmed and stored at 4C. The next day (or few days after) they are permeabilized in 1.5% Triton -PBS overnight at 4C. For staining the micropattern organoids, the same protocol as described above was followed with a few exceptions - Blocking solution was prepared using 10% Normal Donkey Solution, 1% BSA diluted in 0.3% Triton-X in PBS and the organoids were blocked for 2 hours at room temperature followed by Primary antibodies incubation for 24 hours (1:200 dilution in Blocking Solution). Organoids were washed 3x with PBS and Secondary antibodies (1:500 dilution in Blocking solution) and DAPI (1:5000 dilution in PBS) were added and incubated overnight at 4 degrees. (32)

The primary antibodies for immunocytochemistry were diluted as follows: anti-*FOXP1* (abcam, 1:1000), anti-Sox2 (Abcam, ab16288, 1:250), anti-Oct4(Abcam, ab19857, 1:500), anti-Nanog (Fisher Scientific, AF1997, 1:500), anti-Lin28 (CoreBio Services, 3978S, 1:500), anti-N-cadherin (Abcam, ab18465, 1:250), anti-Nestin (Abcam, ab75485, 1:250). Secondary antibodies conjugated to Alexa Fluors 488, 555, 647 were used at a dilution of 1:500 (Life Technologies)

FOXP1 Quantification

Imaris software (Bitplane) was used to quantify FOXP1 positive cells using the ‘add surfaces’ feature.

Clearing

The sample was rinsed in PBT (Phosphate-Buffered Saline with Triton X-100) three times, with each wash lasting 15 minutes. RapiClear was added to the sample and incubated for 1.5 hours to ensure effective clearing.

Micropattern plate single rosette experiment:

Micropatterned plates with 450 μm diameter (4D Cell Technologies, insert catalog number) were coated with matrigel diluted in DMEM/F12 (Life Technologies, 10565042) (1:60 dilution). The plate was incubated at 37 degrees overnight and plated with 3-8M hiPSC cells the next day. N2 media was prepared using 97ml DMEM/F12, 1ml N-2 supplement 100X, 1ml MEM-NEAA, 1ml Pen-Strep 100X, 10 μl β -mercaptoethanol 50mM and the cells were supplemented with ice cold N2 with 4% ice cold matrigel and 5 μM of TGF β -inhibitor SB-431542 the next day. Leave the plates undisturbed the next day and change media on day 4 with N2 + 5uM SB-431542. Starting day 5-9, substitute the N2 media with new N2 media containing 5ng/mL BMP4 and 5 μM of SB-431542. Media is replaced every day and the development is monitored through binocular observation. On day 6, the culture should exhibit a lump in the middle, while on day 7, neural folds should start appearing, and a visible bilayer will emerge.

SUPPLEMENTARY FIGURES

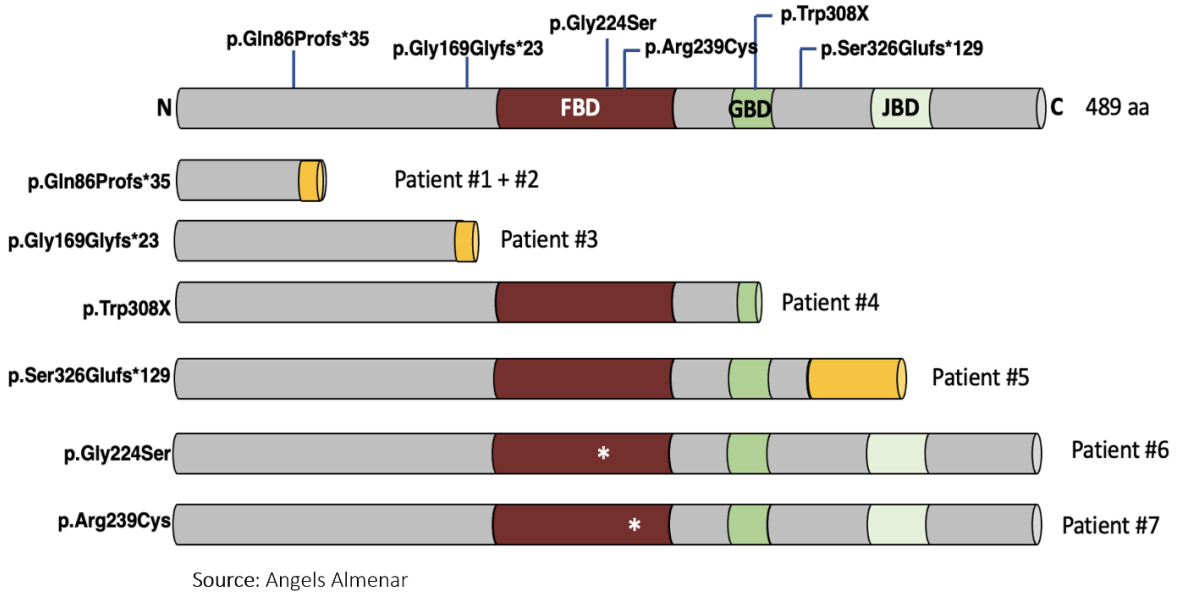


Figure 1: FOXP1 protein map for control line (N) and 6 different FOXP1 mutant lines from 7 different patients. Reproduced with permission.

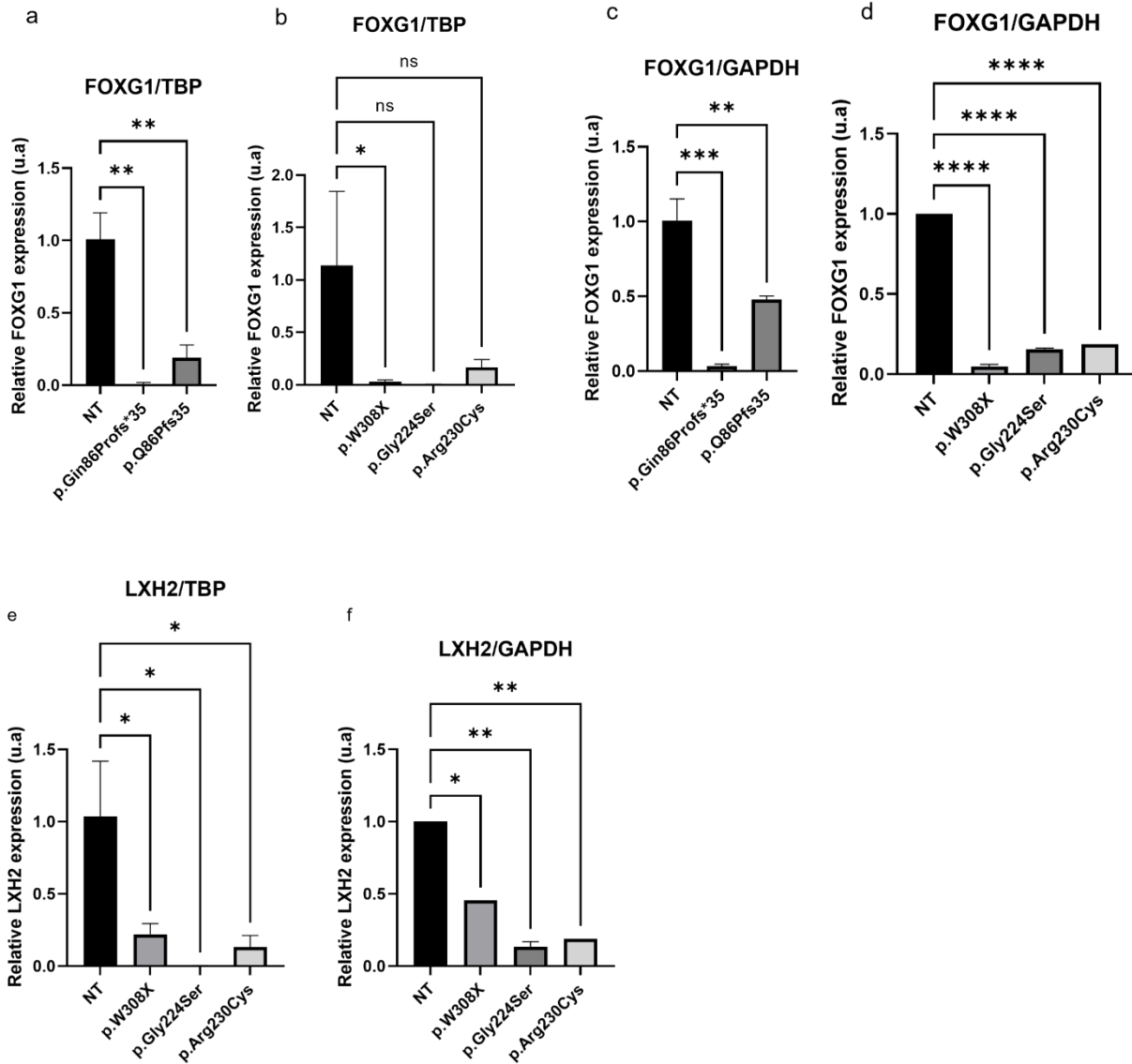


Figure 2: *FOXG1* mutant organoids have lower expression of *FOXG1* as compared to the control organoids. Relative expression of *FOXG1* in 15-day old Control and *FOXG1* mutant patient derived organoids normalized to housekeeping gene a) b) TBP c) d) GAPDH. e) f) Relative expression of *LHX2* forebrain marker normalized to TBP and GAPDH respectively. N = 5 different patient lines, 1 control with 3 replicates each for *FOXG1*. N = 3 patient lines, 1 control with 3 replicates each for *LHX2*.

Size difference after WNTi treatment

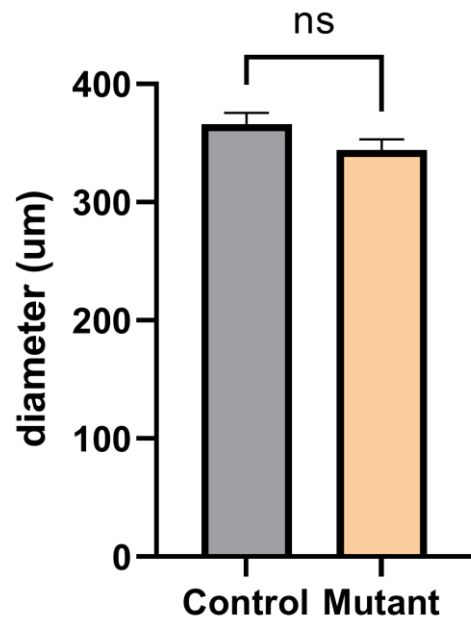


Figure 3: WNT inhibitor treatment may not affect size trend in size between control and mutant organoids. N = 7 patient lines and 1 control line.

SUPPLEMENTARY VIDEOS:

Video 1: Z stack video of control line AG28269B single rosette organoid

https://drive.google.com/file/d/1sQLtS9aSNvquezFP0MIQ7P_7eTYCJttR/view?usp=sharing

Video 2: Z stack video of patient line Gly224Ser single rosette organoid

<https://drive.google.com/file/d/1gQFqapZ9qjkAbJX29t77QNkRn3DDzx1K/view?usp=sharing>

Video 3: Z stack video of patient line Gly224Ser single rosette organoid (replicate 2)

<https://drive.google.com/file/d/1G8acPBQM1bKIJKSop-hZdj5BtQPhJqan/view?usp=sharing>

Video 4: Z stack video of FOXG1 KO line single rosette organoid

<https://drive.google.com/file/d/1-ERhgWyOGg7RUXPWpu8lXRPZepEF9Qeq/view?usp=sharing>

REFERENCES

1. Paving Therapeutic Avenues for *FOXG1* Syndrome: Untangling Genotypes and Phenotypes from a Molecular Perspective. *International Journal Of Molecular Sciences*, 23(2), 954. doi: 10.3390/ijms23020954
2. Akol, I., Gather, F., & Vogel, T. (2022). Paving Therapeutic Avenues for *FOXG1* Syndrome: Untangling Genotypes and Phenotypes from a Molecular Perspective. *International Journal Of Molecular Sciences*, 23(2), 954. doi: 10.3390/ijms23020954
3. FOXG1 foundation website <https://FOXG1research.org/>
4. Xuan, S., Baptista, C. A., Balas, G., Tao, W., Soares, V. C., and Lai, E. (1995). Winged helix transcription factor BF-1 is essential for the development of the cerebral hemispheres. *Neuron* 14, 1141–1152. doi: 10.1016/0896-6273(95)90262-7
5. Younger, S., Boutros, S., Cargnin, F., Jeon, S., Lee, J., Lee, S., & Raber, J. (2022). Behavioral Phenotypes of *FOXG1* Heterozygous Mice. *Frontiers In Pharmacology*, 13. doi: 10.3389/fphar.2022.927296
6. Akol, I., Gather, F., & Vogel, T. (2022). Paving Therapeutic Avenues for *FOXG1* Syndrome: Untangling Genotypes and Phenotypes from a Molecular Perspective. *International Journal Of Molecular Sciences*, 23(2), 954. doi: 10.3390/ijms23020954
7. Xuan S., Baptista C.A., Balas G., Tao W., Soares V.C., Lai E. Winged Helix Transcription Factor BF-1 Is Essential for the Development of the Cerebral Hemispheres. *Neuron*. 1995;14:1141–1152. doi: 10.1016/0896-6273(95)90262-7
8. Trujillo, C., Gao, R., Negraes, P., Gu, J., Buchanan, J., & Preissl, S. (2019). Complex Oscillatory Waves Emerging from Cortical Organoids Model Early Human Brain Network Development. *Cell Stem Cell*, 25(4), 558-569.e7. doi: 10.1016/j.stem.2019.08.002
9. Huang Y, Huang Z, Tang Z, Chen Y, Huang M, Liu H, Huang W, Ye Q, Jia B. Research Progress, Challenges, and Breakthroughs of Organoids as Disease Models. *Front Cell Dev Biol*. 2021 Nov 16;9:740574. doi: 10.3389/fcell.2021.740574. PMID: 34869324; PMCID: PMC8635113.
10. Kadoshima, T., Sakaguchi, H., Nakano, T., Soen, M., Ando, S., Eiraku, M., & Sasai, Y. (2013). Self-organization of axial polarity, inside-out layer pattern, and species-specific progenitor dynamics in human ES cell–derived neocortex. *Proceedings Of The National Academy Of Sciences*, 110(50), 20284-20289. doi: 10.1073/pnas.1315710110
11. Mariani, J., & Vaccarino, F. (2019). Breakthrough Moments: Yoshiki Sasai’s Discoveries in the Third Dimension. *Cell Stem Cell*, 24(6), 837-838. doi: 10.1016/j.stem.2019.05.007
12. Huang, Y., Huang, Z., Tang, Z., Chen, Y., Huang, M., & Liu, H. (2021). Research Progress, Challenges, and Breakthroughs of Organoids as Disease Models. *Frontiers In Cell And Developmental Biology*, 9. doi: 10.3389/fcell.2021.740574

13. Drost, J., van Boxtel, R., Blokzijl, F., Mizutani, T., Sasaki, N., & Sasselli, V. (2017). Use of CRISPR-modified human stem cell organoids to study the origin of mutational signatures in cancer. *Science*, 358(6360), 234-238
14. Huang, Y., Huang, Z., Tang, Z., Chen, Y., Huang, M., & Liu, H. (2021). Research Progress, Challenges, and Breakthroughs of Organoids as Disease Models. *Frontiers In Cell And Developmental Biology*, 9. doi: 10.3389/fcell.2021.740574
15. Wang Y., Jiang T., Qin Z., Jiang J., Wang Q., Yang S. (2019). HER2 Exon 20 Insertions in Non-small-cell Lung Cancer Are Sensitive to the Irreversible Pan-HER Receptor Tyrosine Kinase Inhibitor Pyrotinib. *Ann. Oncol.* 30 (3), 447–455. 10.1093/annonc/mdy542
16. Santos, J., Araújo, C., Rocha, C., Costa-Ferro, Z., & Souza, B. (2023). Modeling Autism Spectrum Disorders with Induced Pluripotent Stem Cell-Derived Brain Organoids. *Biomolecules*, 13(2), 260. doi: 10.3390/biom13020260
17. Gonzalez, C., Armijo, E., Bravo-Alegria, J., Becerra-Calixto, A., Mays, C., & Soto, C. (2018). Modeling amyloid beta and tau pathology in human cerebral organoids. *Molecular Psychiatry*, 23(12), 2363-2374. doi: 10.1038/s41380-018-0229-8
18. Jarazo, J., Barmpa, K., Rosety, I., Smits, L., Arias-Fuenzalida, J., & Walter, J. (2019). Parkinson's disease phenotypes in patient specific brain organoids are improved by HP- β -CD treatment. doi: 10.1101/813089
19. Notaras, M., Lodhi, A., Dünder, F., Collier, P., Sayles, N., & Tilgner, H (2021). Schizophrenia is defined by cell-specific neuropathology and multiple neurodevelopmental mechanisms in patient-derived cerebral organoids. *Molecular Psychiatry*, 27(3), 1416-1434. doi: 10.1038/s41380-021-01316-6
20. Notaras, M., Lodhi, A., Dünder, F., Collier, P., Sayles, N., & Tilgner, H (2021). Schizophrenia is defined by cell-specific neuropathology and multiple neurodevelopmental mechanisms in patient-derived cerebral organoids. *Molecular Psychiatry*, 27(3), 1416-1434. doi: 10.1038/s41380-021-01316-6
21. Xu, Y., Liu, P., Yan, Z., Mi, T., Wang, Y., & Li, Q. (2022). KW-2449 and VPA exert therapeutic effects on human neurons and cerebral organoids derived from MECP2-null hESCs. *Stem Cell Research & Therapy*, 13(1). doi: 10.1186/s13287-022-03216-0
22. Xu, R., Brawner, A., Li, S., Liu, J., Kim, H., & Xue, H. (2019). OLIG2 Drives Abnormal Neurodevelopmental Phenotypes in Human iPSC-Based Organoid and Chimeric Mouse Models of Down Syndrome. *Cell Stem Cell*, 24(6), 908-926.e8. doi: 10.1016/j.stem.2019.04.014
23. Rosebrock, D., Arora, S., Mutukula, N., Volkman, R., Gralinska, E., & Balaskas, A. (2022). Enhanced cortical neural stem cell identity through short SMAD and WNT inhibition in human cerebral organoids facilitates emergence of outer radial glial cells. *Nature Cell Biology*, 24(6), 981-995. doi: 10.1038/s41556-022-00929-5
24. Papes, F., Camargo, A., de Souza, J., Carvalho, V., Szeto, R., & LaMontagne, E. (2022). Transcription Factor 4 loss-of-function is associated with deficits in progenitor

- proliferation and cortical neuron content. *Nature Communications*, 13(1). doi: 10.1038/s41467-022-29942
25. Shimada, H., Sato, Y., Sasaki, T., Shimozawa, A., Imaizumi, K., & Shindo, T (2022). A next-generation iPSC-derived forebrain organoid model of tauopathy with tau fibrils by AAV-mediated gene transfer. *Cell Reports Methods*, 2(9), 100289. doi: 10.1016/j.crmeth.2022.100289
 26. Greber, B., Coulon, P., Zhang, M., Moritz, S., Frank, S., Müller-Molina, A.J., Araúzo-Bravo, M.J., Han, D.W., Pape, H.-C. and Schöler, H.R. (2011), FGF signalling inhibits neural induction in human embryonic stem cells. *The EMBO Journal*, 30: 4874-4884. <https://doi.org/10.1038/emboj.2011.407>
 27. Wang, Y., Chiola, S., Yang, G., Russell, C., Armstrong, C., & Wu, Y. (2022). Modeling human telencephalic development and autism-associated SHANK3 deficiency using organoids generated from single neural rosettes. *Nature Communications*, 13(1). doi: 10.1038/s41467-022-33364-z
 28. Spencer R. Theoretical and analytical embryology of conjoined twins: part I: embryogenesis. *Clinical Anatomy*. 2000;13:36–53. doi: 10.1002/(SICI)1098-2353(2000)13:1<36::AID-CA5>3.0.CO;2-3.
 29. Wang, Y., Chiola, S., Yang, G., Russell, C., Armstrong, C., & Wu, Y. (2022). Modeling human telencephalic development and autism-associated SHANK3 deficiency using organoids generated from single neural rosettes. *Nature Communications*, 13(1). doi: 10.1038/s41467-022-33364-z
 30. Lee, C., Chen, J., Kindberg, A., Bendriem, R., Spivak, C., & Williams, M. (2016). CYP3A5 Mediates Effects of Cocaine on Human Neocortigenesis: Studies using an In Vitro 3-D Self-Organized hPSC Model with a Single Cortex-Like Unit. *Neuropsychopharmacology*, 42(3), 774-784. doi: 10.1038/npp.2016.156
 31. Warmflash, A., Sorre, B., Etoc, F., Siggia, E., & Brivanlou, A. (2014). A method to recapitulate early embryonic spatial patterning in human embryonic stem cells. *Nature Methods*, 11(8), 847-854. doi: 10.1038/nmeth.3016
 32. Karzbrun, E., Khankhel, A., Megale, H., Glasauer, S., Wyle, Y., & Britton, G. (2021). Human neural tube morphogenesis in vitro by geometric constraints. *Nature*, 599(7884), 268-272. doi: 10.1038/s41586-021-04026-
 33. Brenna, C., Simioni, C., Varano, G., Conti, I., Costanzi, E., Melloni, M., & Neri, L. (2022). Optical tissue clearing associated with 3D imaging: application in preclinical and clinical studies. *Histochemistry And Cell Biology*, 157(5), 497-511. doi: 10.1007/s00418-022-02081-5
 34. Hettige, N., & Ernst, C. (2019). FOXP1 Dose in Brain Development. *Frontiers In Pediatrics*, 7. doi: 10.3389/fped.2019.00482
 35. Marchetto MC, Belinson H, Tian Y, Freitas BC, Fu C, Vadodaria K, Beltrao-Braga P, Trujillo CA, Mendes APD, Padmanabhan K, Nunez Y, Ou J, Ghosh H, Wright R, Brennand K, Pierce K, Eichenfield L, Pramparo T, Eyler L, Barnes CC, Courchesne E, Geschwind DH, Gage FH, Wynshaw-Boris A, Muotri AR. Altered proliferation and networks in neural

cells derived from idiopathic autistic individuals. *Mol Psychiatry*. 2017 Jun;22(6):820-835.
doi: 10.1038/mp.2016.95. Epub 2016 Jul 5. PMID: 27378147; PMCID: PMC5215991.